SHRP-S-405

Sprayed Zinc Galvanic Anodes for Concrete Marine Bridge Substructures

Alberto A. Sagüés
Department of Civil Engineering and Mechanics
University of South Florida
Tampa, Florida 33620

Rodney G. Powers
Materials Office
Florida Department of Transportation
Gainesville, Florida 32601

Strategic Highway Research Program
National Research Council
Washington, DC 1994

SHRP-S-405
Contract ID-024
ISBN 0-309-05819-8
Product nos. 2034, 4009

Program Manager: *Kuppusamy Thirumalai*
Project Manager: *H. Martin (Marty) Laylor*
Consultant: *John P. Broomfield*
Program Area Secretary: *Carina S. Hreib*
Production Editor: *Margaret S. Milhous*

key words:

cathodic protection
corrosion
galvanic anode
sprayed zinc
concrete
bridges

Strategic Highway Research Program
National Research Council
2101 Constitution Avenue N.W.
Washington, DC 20418

(202) 334-3774

1.5M/NAP/694

Acknowledgments

The research described herein was supported by the Strategic Highway Research Program (SHRP) under contract no. SHRP-88-ID024. SHRP is a unit of the National Research Council that was authorized by section 128 of the Surface Transportation and Uniform Relocation Assistance Act of 1987.

The work was conducted jointly by personnel of the Materials Office of the Florida Department of Transportation and the Department of Civil Engineering and Mechanics of the University of South Florida. The report was prepared by Alberto A. Sagüés, Rodney G. Powers, Toshiya Murase, and Ivan Lasa.

Contents

List of Tables

List of Figures

Abstract

A low-cost method for galvanic cathodic protection of reinforcing steel in concrete was examined. In this method, arc-sprayed zinc is deposited on the external concrete surface of steel-reinforced marine substructure bridge components, which are normally subject to corrosion of the reinforcement as a result of chloride ion contamination of the concrete. The concrete cover of corrosion-damaged substructure components is removed, exposing the reinforcing steel. After sandblasting, the zinc is arc-sprayed over the exposed steel and surrounding concrete, creating a 1/2 mm thick galvanic anode which is in electronic contact with the steel and in electrolytic contact with the water in the concrete pores. In this investigation, the ability of the system to deliver protective current was examined by experiments in the laboratory and at field installations at bridges in the Florida Keys. The field tests showed that the anodes retained physical integrity over at least 4 1/2 years in a subtropical environment. Typical current densities were 0.5 mA/ft^2 (0.54 $\mu A/cm^2$) on structures containing corroding epoxy-coated reinforcing steel, and 1 mA/ft^2 (1.1 $\mu A/cm^2$) on a plain rebar structure. Steel polarization decay tests with field rebar probes showed that 100 mV polarization decay was routinely achieved. The laboratory tests revealed that in the marine substructure conditions of interest, concrete resistivity does not represent a main limiting factor in the performance of the galvanic anodes. However, absence of direct wetting of the anode surface can result in long-term loss of adequate current delivery, even when the concrete is in contact with air of 85% relative humidity. The results indicate that periodic water contact (as encountered in the splash-evaporation zone of marine bridge substructures) is necessary for long-term anode performance. The method can be viewed as a competitive alternative to impressed-current cathodic protection systems, and also as a considerable improvement over simple gunite repair of corrosion-damaged substructure concrete.

Executive Summary

The substructure of a marine highway bridge is in an aggressive environment. Splash and evaporation of seawater above the waterline causes high chloride ion concentrations in the concrete, followed by corrosion of the reinforcing steel. The corrosion products cause concrete spalling and associated structural damage that often require costly repairs early in the life of the structure. Cathodic protection of the steel can control the corrosion. Conventional impressed-current cathodic protection systems on marine bridge substructures are feasible, but they involve costly anode installations and associated current delivery and control equipment. Sacrificial cathodic protection, by means of sprayed zinc galvanic anodes, is a promising low cost alternative (several times less expensive than impressed current) for protecting these substructures. This project investigated the feasibility of using sprayed sacrificial anodes.

Sprayed zinc anodes can be applied with commonly available metallizing equipment. After the delaminated concrete has been removed, the surface of the spalled concrete and exposed reinforcing steel is cleaned with abrasives and then sprayed with zinc shortly afterward. The electrical connection between zinc and steel is a direct result of the anode application process. Concrete patching is not needed unless required for structural reasons. The cost ranges from \$6 to \$12 per ft^2 (\$65 to \$130 per m^2), according to the job size.

This investigation consisted of field and laboratory activities. The field work determined the physical and electrochemical performance of experimental installations in the Florida Keys. Laboratory experiments were conducted to determine the current deliverability of the anodes, durability, and alternative anode materials, as well as the effect of an organic top-coat.

Field installations were prepared at Florida Keys sites on U.S. Highway 1 at the Bahia Honda, Niles Channel, Long Key, and Seven Mile bridges. Each installation had isolated anode sections that could be used to measure directly the current delivered by the section of anode. Reinforcing steel probes embedded in the concrete indirectly indicated the amount of protection received by the adjacent steel. The performance of the field installations was

monitored over a 2-year period. One of the installations was already 2 1/2 years old at the beginning of this project.

Laboratory experiments used reinforced concrete test columns that were partially immersed in saltwater and small reinforced concrete slabs that had been contaminated with salt. Small sprayed-zinc anodes were applied to the surface of the laboratory specimens, and performance was evaluated by means of electrochemical measurements. Some slabs had pure zinc anodes, and others had 85% Zn-15% Al anodes. The slabs were tested at 25%, 60%, and 85% relative humidity.

Protective current densities on the field installations were typically 1 mA/ft^2 (1.1 $\mu A/cm^2$) on uncoated reinforcing steel assemblies and 0.5 mA/ft^2 (0.5 $\mu A/cm^2$) on piers that had corroding epoxy-coated steel. Polarization decay tests on the reinforcing steel probes had potential decay that typically exceeded 100 mV in 1 hour. Those values are all indicative of reasonable performance. In addition, similar piers in the same bridges that either had been repaired with gunite, or that had no treatment continued to show new corrosion-related damage. The piers with sprayed-zinc anodes have shown no additional cracking since the anodes were installed.

The laboratory test columns had current delivery and polarization values consistent with commonly accepted values for protecting the steel. Anodes in the chloride contaminated region close to the waterline continued to deliver appreciable current after almost 2 years of testing. Anodes on dry, chloride-free noncorroding portions of the columns contributed little to the overall protection current.

Laboratory specimens in the 25% and 60% relative humidity environments showed rapid reduction in protective current delivery with time. The specimens in the 85% environment provided high initial currents but showed rapid decrease of current delivery later. Experiments in which the anode surface was directly wetted by water resulted in sharp current delivery increases. Those experiments, together with the field observations, suggest that direct wetting of the anode (by seawater splash or spray) may be a necessary factor in obtaining adequate protection.

The alternative 85% Zn-15% Al anode appears to provide added driving potential compared with commercially pure zinc.

There was no conclusive evidence that topcoating the anodes changed their electrochemical performance.

The results indicate that the sprayed anodes perform well in the splash zone of marine bridge substructures, where corrosion protection is most needed. The system can be considered a low-cost maintenance alternative to gunite patch repairs, which develop further corrosion-related damage after as little as 2 years of service.

If long-term durability is established by further monitoring, the system may be a competitive alternative to impressed-current cathodic protection.

1

Introduction, Objectives, and Approach

1.1 Introduction

1.1.1 Corrosion Control in Marine Substructures

Severe corrosion damage often affects reinforcing steel in the substructure of highway bridges exposed to marine environments. Reinforcing steel, which is initially passive in chloride-free concrete, experiences active corrosion upon contact with chlorides.[1] In marine substructures, the chloride from the environment permeates through the concrete. Chloride transport to the reinforcing steel surface takes place not only by diffusion, but also by capillary convection. This is facilitated by water evaporation at the upper portions of the substructure and by cyclic wetting and drying of the concrete at the tidal and splash zones.[2,3] When those zones are exposed to subtropical environments, it is not uncommon to encounter chloride levels exceeding 10 pounds per cubic yard (pcy) (1 pcy = 0.59 kg/m^3) at a depth of 2 in. (5.1 cm) below the concrete surface after 5 to 10 years of service. Under these conditions, substructure elements typically need repair after 12 to 15 years of service.[4] The severity of that environment is underscored by recent observations of widespread deterioration of epoxy-coated reinforcing steel in Florida substructures.[5]

Current repair practice is often limited to patching the spalled region with new concrete. Even if the new concrete is designed for low chloride penetration, corrosion is likely to proceed at adjacent regions, requiring repair there within a few years. Repeated repairs are costly and do not provide a lasting solution to the problem.

Cathodic protection with impressed-current anodes can be used to stop the progression of damage. While this method can provide positive protection, implementation on a marine bridge substructure is much more complex than on a superstructure. For example, concrete conductivity varies widely with the height above water, and tidal action can create large periodic variations in current distribution. The mechanically aggressive environment can

wash away conductive polymeric coatings. Elaborate anode configurations may be required to ensure reliability under these conditions.[6,7] In the case of corroding epoxy-coated reinforcing steel, conventional cathodic protection would require individual electrical connections to each steel element, a cumbersome and possibly impracticable task. These factors have resulted in relatively little use of impressed-current systems for protecting reinforcing steel in marine substructure applications in the United States. At present, projected costs are large, and therefore widespread application is discouraged.

1.1.2 Nature of the Innovation Investigated

An intermediate approach between replacement repair and costly impressed-current systems is highly desirable. The investigation described here was conducted to develop and establish the performance of an alternative based on the use of sprayed zinc as a galvanic anode.

Zinc is used extensively in galvanic anode service because of its low position in the standard (EMF) table (-0.763 V versus SHE), relatively low price, availability, environmental compatibility, and ease of handling. Because zinc can be sprayed on the surface of concrete, it forms an anode ideally shaped to maximize contact with the concrete and be as close as possible to the metal to be protected. Electrical contact between the reinforcing steel and the zinc anode is achieved either by a connecting wire, or more conveniently, by direct spraying of zinc on the exposed reinforcement. The latter procedure is particularly suited to the common morphology of damage, where some reinforcement is often exposed.

Before the zinc is applied, the delaminated concrete is removed and the surface of the affected member is sandblasted. The concrete and steel reinforcement surfaces are thus thoroughly cleaned and roughened, improving adhesion of the sprayed metal.

In the case of corroded epoxy-coated reinforcing steel, the initial blasting easily removes the polymer coat and underlying corrosion products. For epoxy-coated material the protection provided by this method covers, in principle, only those bars directly in contact with the sprayed zinc. However, the straight bars in a typical substructure column extend vertically over most of the region affected by corrosion, while circularly bent bars extend around the column. A typical spall often exposes as much as one third to one half of the steel segments experiencing severe corrosion.

The zinc application involves all exposed bars at once; consequently, the process is much less labor- and time-consuming than using individual electrical connections. In addition, the zinc spray contacts each bar over the entire exposed area, establishing continuous redundant connections.

The application process has been successfully conducted in previous field trial installations on substructure columns where epoxy-coated reinforcing steel was extensively corroded.

The spray gun uses an electric arc sustained at the end of continuously fed zinc wires, operating typically at 25 V, 250–350 A (DC). Compressed air atomizes the zinc and deposits the droplets onto the working surface. Application is straightforward and quick. Usually two to three passes are sufficient to deposit a suitable zinc layer (0.016 in. [0.4 mm] thick, about 90% dense) at a rate of 2 ft^2 (0.19 m^2) per minute. Commercial equipment and operators are readily available for this procedure. The equipment permits easy access to the job location. Complex shapes and surfaces in any orientation can be covered effectively.

Current costs for experimental installations corresponded to typical installed costs (including surface preparation, etc.) of \$6 to \$12 per ft^2 (\$65 to \$130 per m^2), compared with approximately \$40 per ft^2 (\$430 per m^2) for conventional impressed-current cathodic protection systems on marine substructures, based on experience of the Florida Department of Transportation (DOT).

1.1.3 Previous Work in Related Areas

While impressed-current methods for cathodic protection of steel in concrete were the subject of much development in recent years, the use of sacrificial anodes has been limited.[8,9,10] In a pioneering U.S. investigation, Whiting and coworkers[11] explored the use of sacrificial zinc anodes to protect an interstate highway bridge deck. The anodes were either solid metal strips or perforated sheets. The anodes were embedded in mortar, which in turn was covered with a 2 in. thick layer of asphaltic concrete. Wearing surface potential shift measurements showed that requirements for protection were approached on two of the three bridge spans tested. The current delivery of the system depended on seasonal conditions, which affected the resistivity of the concrete.

Sacrificial embedded aluminum alloy anodes have been used experimentally in tropical environments in Venezuela to protect bridge pilings[12]; this application required the use of a permeable concrete cover over the anode to allow anode reaction products to dissipate.

External galvanic anodes to protect the submerged portion of substructures have been proposed and used,[13,14] but their efficiency in the tidal or splash zones is limited.[14]

Metallizing (sprayed-metal) technology for impressed-current anodes on atmospherically exposed concrete was initially investigated by the California DOT (Caltrans).[15] The California work included extensive laboratory tests to select anode materials suitable for concrete in terms of applicability, durability, and cost. Zinc metallizing was identified as one of the methods that best met the selection criteria.

A zinc-metallized substructure column was tested in impressed-current service for several years at the Richmond–San Rafael Bridge in San Francisco Bay. The study demonstrated that metallized coatings can be successfully applied to a large structure and remain in service for extended periods of time under field conditions. Other applications of this concept have since been successfully implemented, for example in Oregon.[16]

The initial California system required rectifier power (3 to 6.3 V) to provide the desired current levels. While the substructure member tested was part of a bridge in marine service, the height over the water and the environmental conditions were such that concrete resistivity was high. The anode-to-steel resistance of the coated segment closest to the water (approximately 50 ft^2 (4.7 m^2) of concrete surface, and 30 ft^2 (2.8 m^2) of reinforcing steel surface) was reported to be in the 100 to 600 ohm range.[15] Steel-to-surface resistance measurements prior to metallizing indicated that the concrete was the major contributor to the resistance. Assuming a typical concrete cover of 2 in. (5.1 cm), the results indicate that the effective concrete resistivity at the lowest column level (closest to the water) exceeded 10^5 ohms-cm.

Preliminary laboratory and field trials of galvanic sprayed-zinc anodes, using the concept investigated here, were conducted by the Florida DOT in 1988/89.[17] In the field tests, substructure columns were coated on the Niles Channel bridge, a Florida Keys location where extensive epoxy-coated reinforcing steel corrosion has been observed. The underdeck of the Julia Tuttle Causeway bridge near Miami was also coated. Initial experience showed that the installations had survived over 1 year without significant deterioration. Polarization decay tests on small reinforcing steel probes embedded in the concrete gave results that exceeded the commonly used 100 mV polarization decay criterion for protection.[17]

The preliminary laboratory tests in Florida used zinc-sprayed cylindrical specimens of steel in concrete. The findings concurred with the field results and showed polarization decays in excess of 100 mV after current interruption.

Previous experience at Florida sites using conventional cathodic protection systems showed that effective concrete resistivities are as much as one order of magnitude lower than in the impressed-current California tests mentioned earlier. This is expected because of the high humidity and high temperature environmental conditions prevalent in Florida. The encouraging preliminary findings in Florida led to proposing and executing the present work.

1.1.4 Research Needs Addressed by This Investigation

The ability of a system to deliver the required levels of protective current is critical to the success of cathodic protection. Experiments were needed to establish the range of service conditions where the system provides adequate protective current.

Metallizing allows the use of different alloy compositions. The initial Florida tests used commercially pure zinc, but other alloys may provide better performance, and it was important to investigate the performance of alternative anode compositions.[18-21]

Zinc coatings have shown good durability in long-term tests in marine service. Coatings that are 0.01 in. (0.3 mm) thick have provided adequate protection to steel substrates in 19-year tests of severe marine exposure.[22,23] While recent measurements of zinc performance in subtropical environments provided additional criteria for selecting coating thickness,[24] the

performance of metallized coatings on concrete was less documented,[22] and further durability testing was needed.

The service life of metallized zinc anodes on concrete also depends on the metal-concrete interface phenomena. Moist concrete presents an alkaline environment, and if the Ph exceeds 12.5, high zinc corrosion rates may occur.[23,25] These could be reduced by anodic action and residual atmospheric access, which tend to reduce the surface Ph (compared with a fully embedded anode). The extent of these effects was unknown.

Another possible problem was the accumulation of metal dissolution products at the zinc-concrete interface. This could increase the circuit resistance and promote delamination of the anode. Reduction of current delivery with time was observed at the California field tests and was attributed to the accumulation of corrosion products.[15] These factors needed further investigation and were addressed in the investigation described in the following sections.

1.2 Objectives

The purpose of this investigation was to assess the performance of zinc-metallized anodes as a cost-effective galvanic anode for controlling corrosion of reinforcing steel in marine substructures, and to obtain information needed for routine anode application in the field.

Three major research objectives were identified:

- Determine whether the metallized zinc anodes could provide the required levels of current for protection.
- Determine the effect of service and application parameters on the durability of the metallized anodes.
- Establish the applicability of the method under field conditions.

1.3 Approach

The first two objectives were addressed by means of laboratory experiments using chloride-contaminated reinforced concrete specimens on which anodes were sprayed. Most specimens were in the form of small slabs. These specimens were exposed in low, intermediate, and high relative humidity environments. Current delivery was studied by operating under simple galvanic coupling. Durability was examined by impressing controlled current densities and determining the changes in required driving voltage as a function of time.

Selected specimens were coated with a weatherproofing compound to establish the possible effect on durability and performance.

Two different sprayed metal formulations (commercially pure zinc and 85% Zn-15% Al) were compared. The distribution of current under simulated substructure conditions was evaluated by means of columnar specimens partially submerged in saltwater.

The third objective was addressed by installing and evaluating sprayed-zinc anode systems on selected bridge substructure components in Florida. Current delivery and other performance tests were conducted.

2

Procedure—Laboratory Experiments

2.1 Compact Test Specimens (Slabs)

The base configuration of the slabs was designed as shown in Figure 2.1. The zinc patch was designed to have a 1:1 zinc-to-steel surface ratio. Each slab contained a centrally placed embedded reference electrode. The base configuration and variations used are listed below and in Table 2.1.

A0 Base configuration as in Figure 2.1. These single-bar-mat specimens were tested in the normally connected condition.

A1 As in A0, but with an activated titanium mesh (Elgard anode mesh), instead of reinforcing steel, to impress a controlled anodic current density on the sprayed anode.

A2 Base configuration, but without connection between the reinforcing steel and the zinc anode; used as control specimens.

A3 As in A1, but with the anode split into two different patches (zinc and zinc-aluminum) and no topcoat.

A4 As in A3, but with organic topcoat over the sprayed anode.

The concrete used for the slabs was made with Type II cement, standard Florida DOT aggregates (with maximum size restricted to 3/8 in. [1 cm]) and a water-to-cement ratio of 0.45. Table 2.2 lists the concrete mix proportions. The slabs were removed from their molds after 4 weeks of curing. The specimens were allowed to dry in laboratory air for 2 weeks before starting the salting procedure.

Table 2.1

Compact Test Specimens
Test Conditions and Number of Specimens per Condition

Specimen Type (See section 2.1)	Test Environment Relative Humidity		
	25%	60%	85%
A0 (base)	3	3	6
A1 (single, 1 mA/ft^2)	-	-	3
A2 (control)	-	-	3
A3A (dual, 1 mA/ft^2)	3	-	3
A3B (dual, 10 mA/ft^2)	-	-	3
A4A (dual, organic-coated, 1 mA/ft^2)	-	-	3
A4B (dual, organic-coated, 10 mA/ft^2)	-	-	3

1 mA/ft^2 = 1.1 μA/cm^2

The specimens were placed in a covered stainless steel tank and subjected to daily 1-hr showers with 15% NaCl solution over a period of 40 days. Ambient outdoor air was circulated through the tank except during each salt spray. An internal electrical heater was used to achieve inner tank air temperatures that were typically 5°C higher than external air (which was under typical summer weather conditions). To further accelerate chloride ingress in the slabs, four short holes (0.5 in. diameter [1.3 cm], 1 in. [2.5 cm] deep) were drilled on the face of the slab closest to the reinforcing steel. The holes were evenly placed so that they would reach between the reinforcing steel bars but not directly expose metal. The holes were plugged with mortar after the salting procedure was completed.

The arc-spray metal application was performed by Restly Marine Service, using procedures and equipment similar to those used by the same company on the Julia Tuttle Bridge (in the Miami area). The zinc wire was 99.9% pure. The coating had a typical thickness of 0.018 inches (0.46 mm). The arc spray gun was operated at 300–325 A, 25 V. The commercially pure zinc patches were applied, and isolated strips of zinc were sprayed on the same face as the main patch to provide pulloff test spots for measuring bond strength.

The alternative alloy chosen for the A3–A4 specimens was 85% Zn-15% Al. This material was chosen for its availability and for comparison with research presently sponsored by the International Lead-Zinc Research Organization on the durability of this alloy as impressed-

Table 2.2

Concrete Mix—Compact Laboratory Specimens

Design:	
Cement Type:	II
W/C Ratio:	0.45
Fine Aggregate:	1140 pcy
Coarse Aggregate:	1812 pcy
Cement Factor:	582 pcy
Slump Range:	3–6 in.
Air Content:	5%

1 pcy = 0.59 kg/m^2
1 in. = 2.54 cm

current anodes on concrete. Due to equipment malfunction near the end of the scheduled workday, only 2 of the 12 85% Zn-15% Al metallized specimens were prepared initially; the rest were prepared 2 months later.

An exposure chamber was constructed for the specimens to be tested in the high moisture environment. The 6 ft × 3 ft × 1.5 ft (1.8 m × 0.9 m × 0.45 m) enclosure permitted external electrical connections to each specimen. Humidity was manually controlled to achieve 85% (± 5%) relative humidity. The laboratory air used to expose selected Type A0 specimens had an average humidity of approximately 60%. The low-humidity tests were conducted in a chamber with an average humidity of approximately 25%.

An organic top coat (Texcote XL-70) was applied over the metallized surfaces of the Type A4 specimens after about 100 days of exposure in the 85% humidity chamber.

The following tests were performed on the specimens.

2.1.1 Galvanic Current Delivery

The current between the anode and the reinforcing steel (or the titanium electrode in the impressed current tests) was measured with a 5 ohm input resistance ammeter (Fluke Model 27 in the mA range).

2.1.2 Instant-Off Potentials

The potentials of the anode and reinforcing steel (or the titanium electrode in the impressed current tests) of the normally connected specimens were measured 1 second after current interruption, with respect to the internal reference electrode. In specimens with dual anodes, all currents were interrupted simultaneously. All potential measurements were conducted with voltmeters with an input resistance of 10 MΩ or higher.

The internal reference electrodes were calibrated periodically against an external copper-copper sulfate electrode (CSE) with the anode-to-steel current off.

The potentials in the control specimens were determined in their normally off condition.

2.1.3 Inter-element Resistance

Figure 2.2 illustrates these resistance measurement procedures. With all currents off, a soil resistance meter (Nilsson Model 400, 97 Hz square wave alternating current) was used to measure the resistance between the reinforcing steel (or the titanium electrode in the impressed current tests) and the anode.

With the meter set in a three-point configuration, the resistance between the anode and a parallel plane containing the reference electrode, or, alternatively, the resistance between the steel and the plane, was determined. As the reference electrode was normally placed midway between the bars and the anode, the results of these partial resistance measurements are called "anode-to-midpoint" resistance and "steel-to-midpoint" resistance throughout this report.

2.1.4 Polarization Decay

The current in the specimens was turned off, and the potentials of the reinforcing steel and the anode were determined after 1 second, 1 minute, 10 minutes, 1 hour, 4 hours, and longer periods when desired. The connection between bar and anode was reestablished after the test was completed.

2.1.5 Polarization Diagrams

These tests attempted to establish the electrochemical characteristics of the steel and anode material. In the control specimens, the E-log i behavior of anode or reinforcing steel was determined using a potentiodynamic method, starting from the open circuit potential and deviating in the cathodic direction (for reinforcing steel) or the anodic direction (for the anode) at a low rate (for example, 0.05 mV/sec). The scan amplitude was 300 mV for the

cathodic scans and 200 mV for the anodic scans. The tests were performed with a computer-controlled PAR Model 273 potentiostat, operating in the IR compensated mode.

2.1.6 Microstructural Examination

The microstructure around the zinc-concrete interface of selected specimens was examined. Small cores, 10 mm in diameter and 10 mm deep, were removed from the specimen. After being embedded in an epoxide resin, the cores were sliced longitudinally with a diamond saw. The exposed cross section was further impregnated with epoxide and polished using standard metallographic procedures. A metallographic microscope was used to examine the cross sections.

2.1.7 Surface Wetting Tests

After the current stabilized, selected specimens were wetted by applying a distilled water-saturated sponge to the center of the anode surface, minimizing wetting of the anode edges. The current delivery and electrode potentials were monitored for various periods of time afterwards. The procedure was repeated for several cycles.

2.2 Instrumented Test Columns

The columns were designed as shown in Figure 2.3. The columns were 48 in. tall, 12 in. wide, and 4 in. thick (122 × 30 × 10 cm). Horizontal #6 steel segments, with an effective length of 8 in. (20.3 cm), were placed in groups of three bars at various heights. The portion of the column containing the two lowest groups of bars was made of concrete containing 20 pounds per cubic yard (pcy) (12 kg/m^3) chloride ion. The three highest groups were in chloride-free concrete. The waterline was positioned so that only the lowest group was fully immersed. The chloride and water distributions were intended to represent typical marine substructure exposure. Sprayed zinc was applied in patches over each of the four highest groups of bars. The bar and patch dimensions were set to obtain a 1:1 zinc-to-steel surface ratio. Internal reference electrodes were embedded facing the center of each reinforcing steel group. The wiring schematic is shown in Figure 2.4. Longitudinal fiberglass reinforcing bars were placed to avoid accidental cracking during handling of the columns.

The columns were cast in March 1991. The concrete used was Type I cement, standard Florida DOT aggregates (maximum aggregate size was set to 3/8 in. [1 cm] for these columns) and a water-to-cement ratio of 0.45. The chloride ions in the lower portion of the column were added by mixing in the appropriate amount of NaCl. A removable dam divided the upper and lower portions of the column during casting; the dam was removed after the concrete was completely consolidated. Table 2.3 shows the concrete mix design proportions.

Table 2.3

Concrete Mix—Laboratory Columns

Design:	
Cement Type:	II
W/C Ratio:	0.45
Fine Aggregate:	1140 pcy
Coarse Aggregate:	1812 pcy
Cement Factor:	582 pcy
Slump Range:	3–6 in.
Air Content:	5%

(Above data for upper portion of the column. 20 pcy Cl^- were added as NaCl to the lower portion.)

1 pcy = 0.593 kg/m^2
1 in. = 2.54 cm

The columns were cured for 4 weeks before being removed from their molds. After approximately 1 week of air-drying, the columns were placed vertically in a tank containing a 5% NaCl solution, with only the lower 10.5 in. (27 cm) immersed. All the bar segments were short-circuited in each column at that time.

The columns were removed from the tank after 40 days, and the anodes were installed the next day. The columns were returned to the tank 1 week later.

The following tests were performed.

2.2.1 Inter-element Currents

Figure 2.4 shows a schematic of the connections between the anodes and bars. Switches 1 to 8 were kept normally closed; a 5 ohm input resistance meter was periodically used to measure the currents through the switches. The electronic currents leaving each anode (I_{Zn1} to I_{Zn4}) and entering each reinforcing steel group (I_{B1} to I_{B5}) were calculated by the difference between the currents measured at the switches above and below the reinforcing steel group.

2.2.2 Instant-Off Potentials

The entire set of switches for the column was turned off at once, and potentials readings between each element and the closest reference electrode were taken within 1 second.

2.2.3 Inter-element Resistance

The anode-to-adjacent bars resistance was periodically measured by opening all switches and using an AC soil resistance meter. Three-pin measurements similar to those shown in Figure 2.2 were also performed to determine anode- and steel-to-midpoint resistances.

2.2.4 Polarization Decay

The entire set of switches for the columns was turned off, and potentials with respect to the closest reference electrode of each element were taken over an interval of several hours.

2.2.5 Surface Wetting

A procedure similar to that used for the compact specimens was used after a stable current flow had developed in the columns.

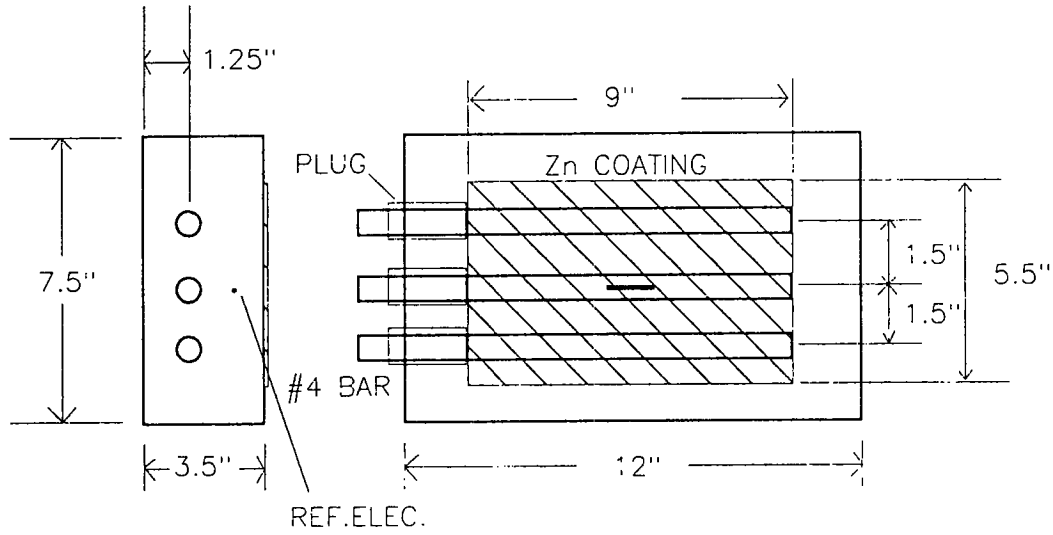

Figure 2.1 Base configuration of compact test specimens (1 in. = 2.54 cm)

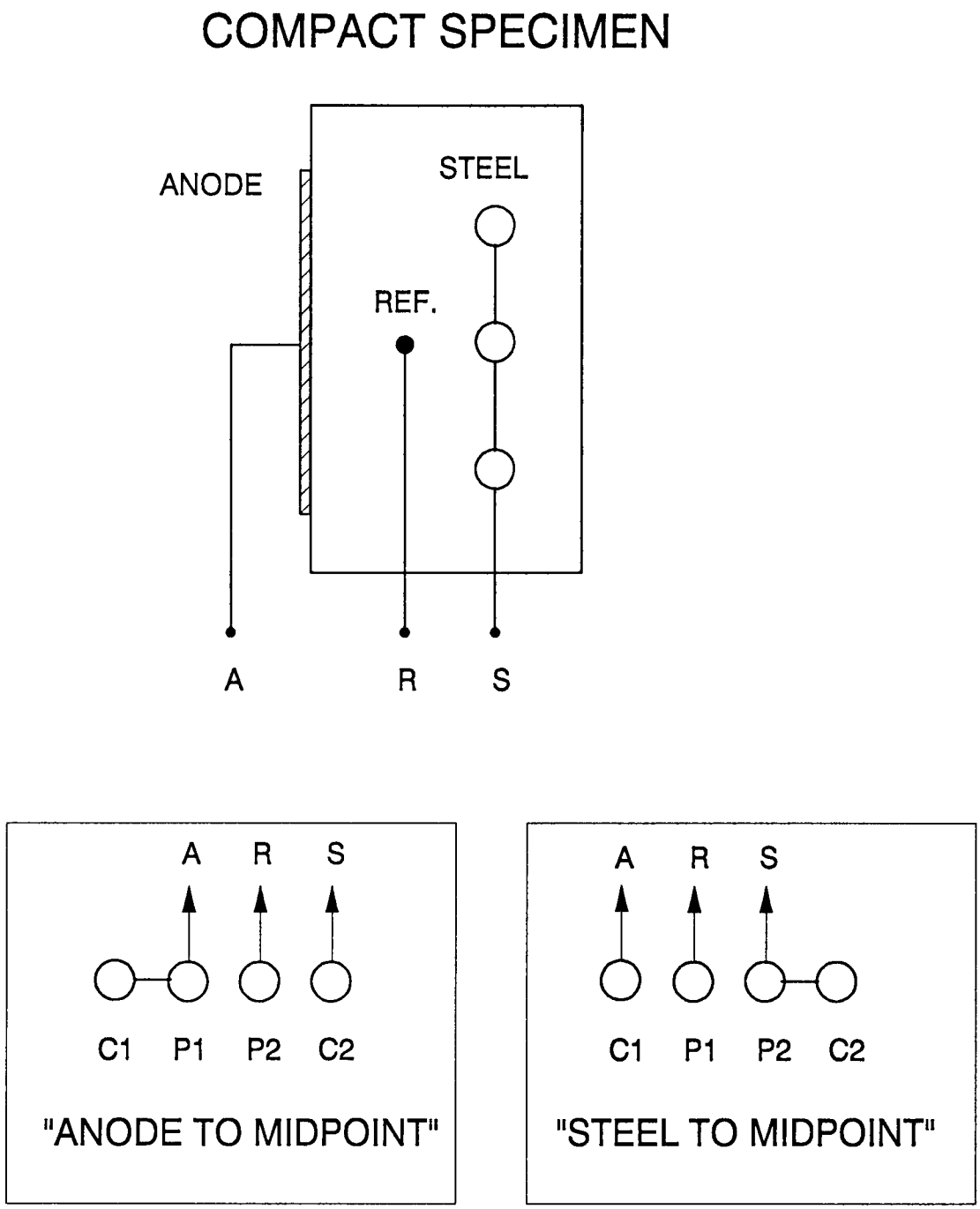

Figure 2.2 **Connections of soil resistance meter used to measure "anode to midpoint" and "steel to midpoint" resistances. C1, C2 and P1, P2 designate current and potential terminals respectively of the Nilsson 400 meter.**

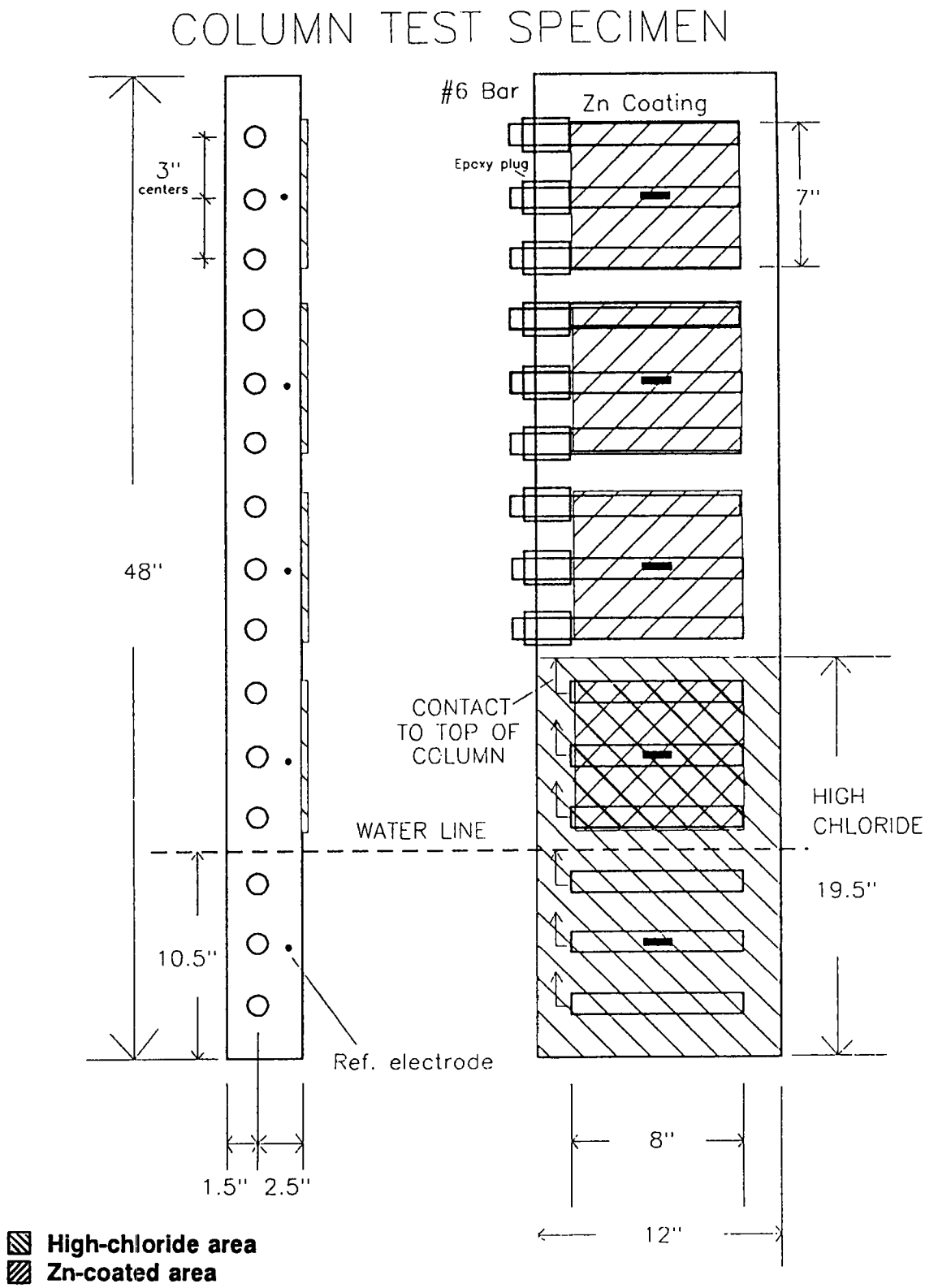

Figure 2.3 Instrumented test column (1 in. = 2.54 cm)

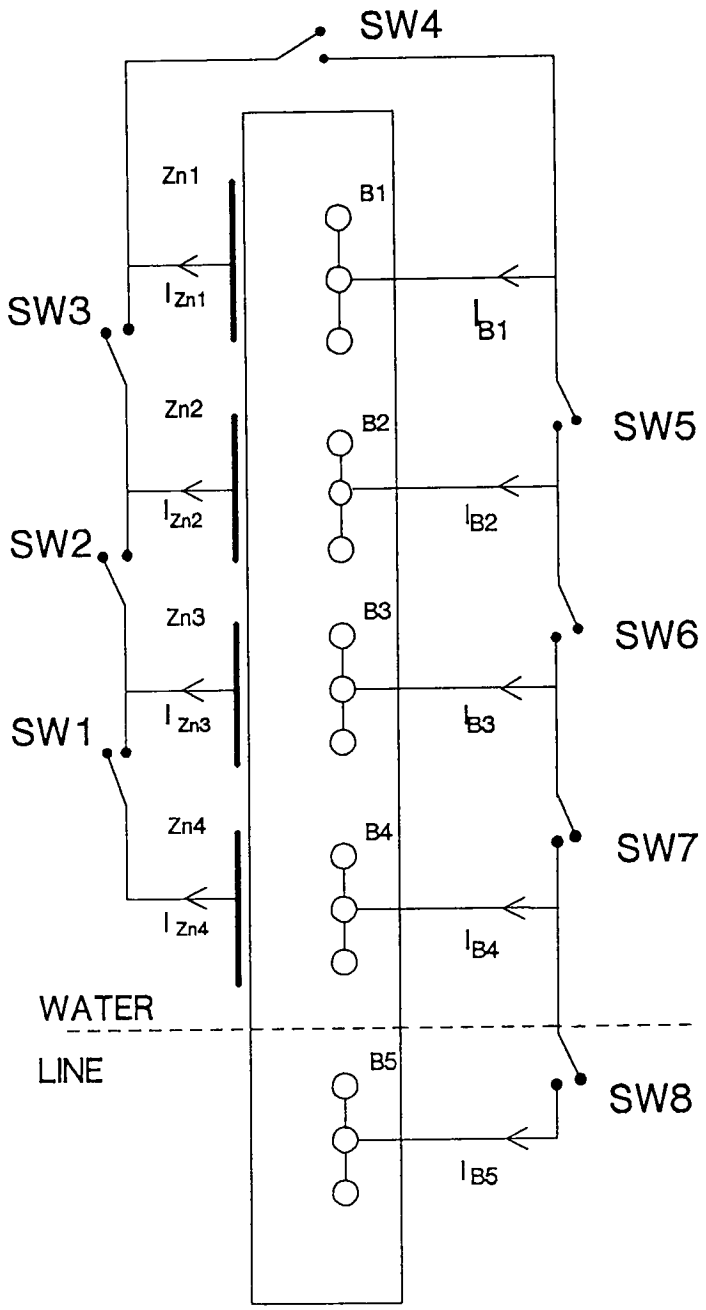

Figure 2.4 **Schematic connection of the instrumented test columns. Electronic currents flowing in the direction of the arrows are defined as positive.**

Procedure—Field Investigations

3.1 Site Selection

Four structures in the Florida Keys were selected for application and evaluation of sprayed zinc anodes (Bahia Honda Bridge, Long Key Bridge, Niles Channel Bridge, and Seven Mile Bridge; see Table 3.1). All structures are located on U.S. Highway 1. The Bahia Honda Bridge had plain rebar and showed severe corrosion spalling. The other three structures contained epoxy-coated rebar and had experienced severe corrosion damage.[4,5] The Niles Channel Bridge had been previously metallized in November 1988, thus providing a site for gathering long-term performance information within the short duration of this project.

The structures varied in age at the beginning of the study, from 22 years (Bahia Honda) to about 11 years (the three other bridges). The sites selected offered the opportunity to evaluate the sprayed zinc anode on both epoxy coated and plain reinforced concrete elements. Figures 3.1 through 3.4 show the structure and test site configurations.

3.2 Application of the Sprayed Zinc Anode

Superior Arc Metallizing Co. of Mobile, Alabama, was contracted by the Florida Department of Transportation (DOT) to apply the sprayed zinc anode to the test sites at Bahia Honda, Seven Mile, and Long Key Bridges. This contractor was selected on the basis of competitive bidding and prior Florida DOT experience. The total cost of the installation was $4,788, paid by Florida DOT under the cooperative features of the Strategic Highway Research Program–IDEA proposal and contract.

The first step in preparing the surface was to remove mechanically the delaminated concrete; the exposed steel and the surrounding concrete surface that was to receive the sprayed zinc anode was then blasted clean (with grade 20–30 silica sand). Conventional

Table 3.1
Sprayed Zinc Anode Test Sites
U.S.-Highway 1, Florida Keys

Date Metallizing	Bridge Name	Location Mile Marker	Rebar*	Components Tested	Pier Nos.	Approx. Area (sq. ft)	Age (yrs)
11/15/88	Niles Channel	29	E	Columns (2)	5, 33	100	11
04/16/91	Bahia Honda	42	P	Footer, Column	29	180	22
04/17/91**	Seven Mile	45	E	Column	5	60	12
04/18/91	Long Key	63	E	Cap	56	250	11

* E = Epoxy Coated, P = Plain Rebar
**Remetallized January 1992

blast cleaning equipment was used, powered by a 200 ft^3/min (5.7 m^3/min), 250 psi (1.7 MPa) compressor. Exposed bars were cleaned to near white (SSPC-10), and the surrounding concrete was lightly blasted to a "color change" condition. The "color change" condition is a reliable criterion for ensuring surface cleanliness, provided both the sand and concrete are dry.

Immediately after the sandblasting and just before application of the sprayed zinc anode, the concrete surface was blown down with air to remove residual debris. The zinc was applied with conventional arc metallizing equipment. The gun was held 10 to 14 in. (25 to 36 cm) from the surface.

Zinc wire is supplied in 500 ft (150 m) rolls. Direct current (DC) was supplied with a standard welding rectifier rated to 600 A, 44 V. Air pressure for the metallizing gun was supplied by the sandblasting equipment. The metallizing equipment was operated at 250–300 A, 25 V.

The zinc was applied in multiple passes to yield a coating thickness of approximately 0.016 in. (0.4 mm). Coating thickness measurements were taken with a round anvil micrometer by measuring the thickness of zinc samples obtained from duct tape placed on the column prior to metallizing.

3.3 Instrumentation

Each test site was instrumented so that anode and cathode current and potential could be measured. Reinforcing steel probes were embedded in each of the sites to allow measurements of current delivery and potential shifts. The probes were lengths of 0.5 in. (1.3 cm) diameter reinforcing bars with an exposed area of 2 $in.^2$ (13 cm^2). Each probe had a length of insulated copper wire mechanically fastened and sealed at one end of the probe. The probes were embedded in a sand-cement mortar (mixed using seawater), and the wire extended out of the surface to facilitate easy connection to the zinc anode.

The probes were placed in pairs spaced vertically along the length of the metallized area to allow for both polarization and depolarization tests during monitoring (Figures 3.1 through 3.4). To permit measurements of anode current density, 1 ft^2 (0.93 m^2) windows were first isolated by saw cutting at elevations corresponding to the probes. A 3/4 inch (2 cm) wide stainless steel band was used to provide continuity between the window zinc to the surrounding zinc anode and to provide convenient means for connecting or disconnecting the window during testing. Methods of testing are detailed further in Chapter 5.

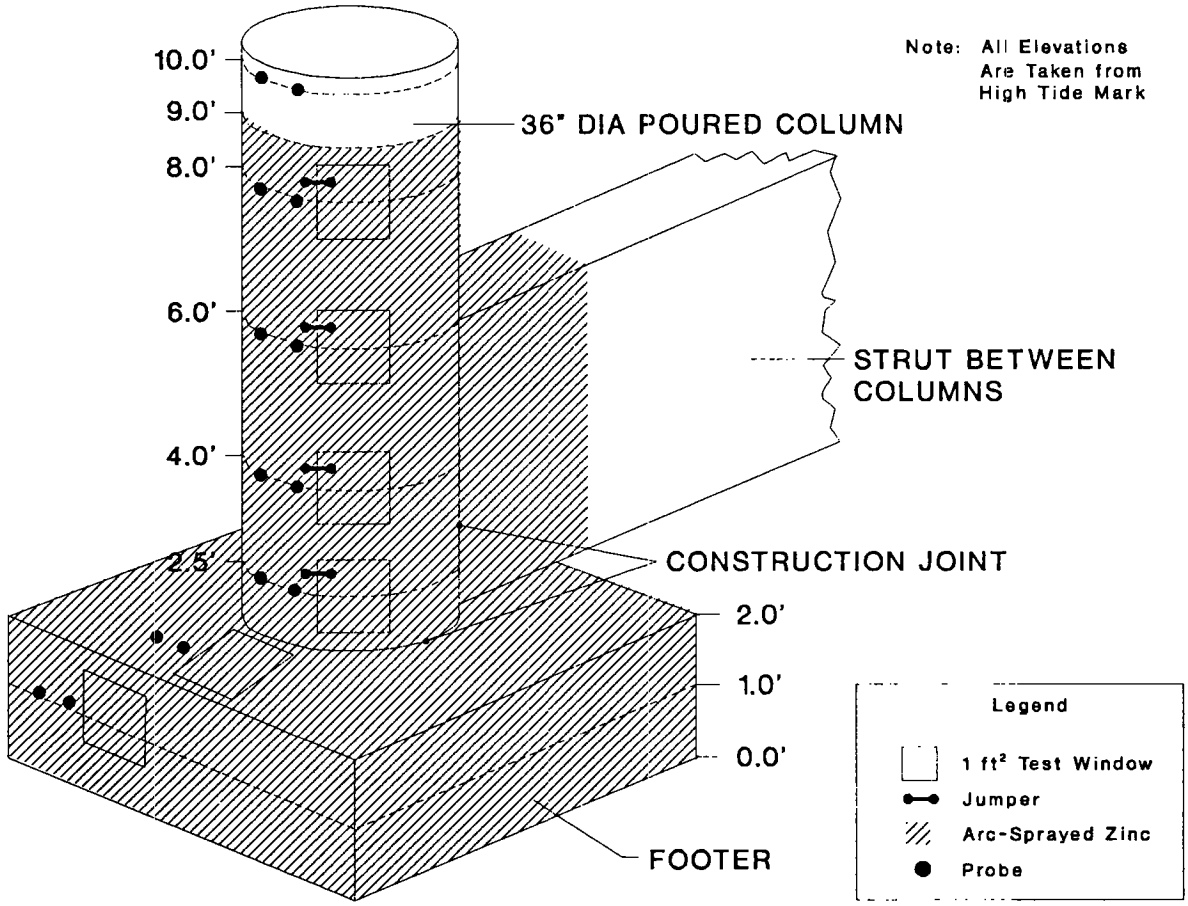

Figure 3.1 Schematic of test site at Bahia Honda Bridge (1 in. = 2.54 cm; 1 ft = 30.5 cm)

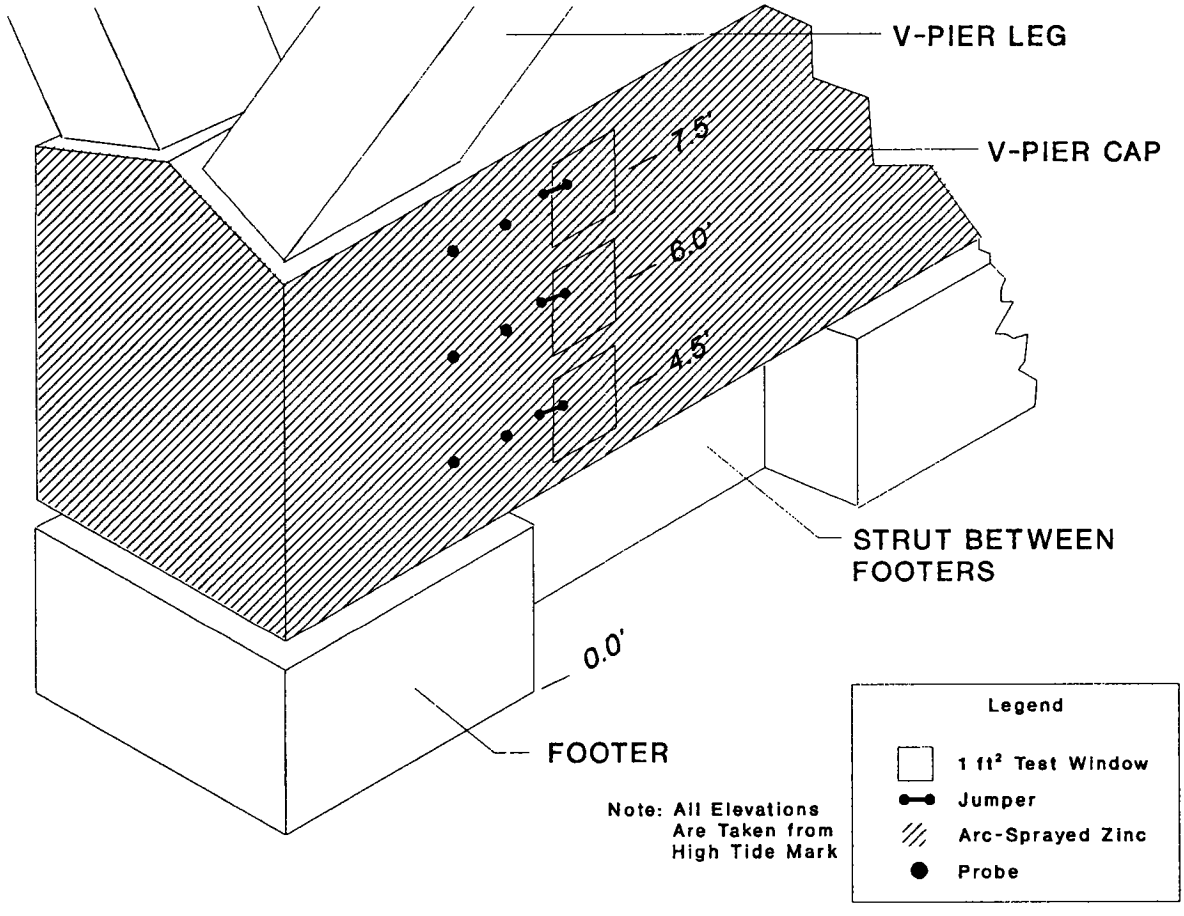

Figure 3.2 Schematic of test site at Long Key Bridge (1 in. = 2.54 cm; 1 ft = 30.5 cm)

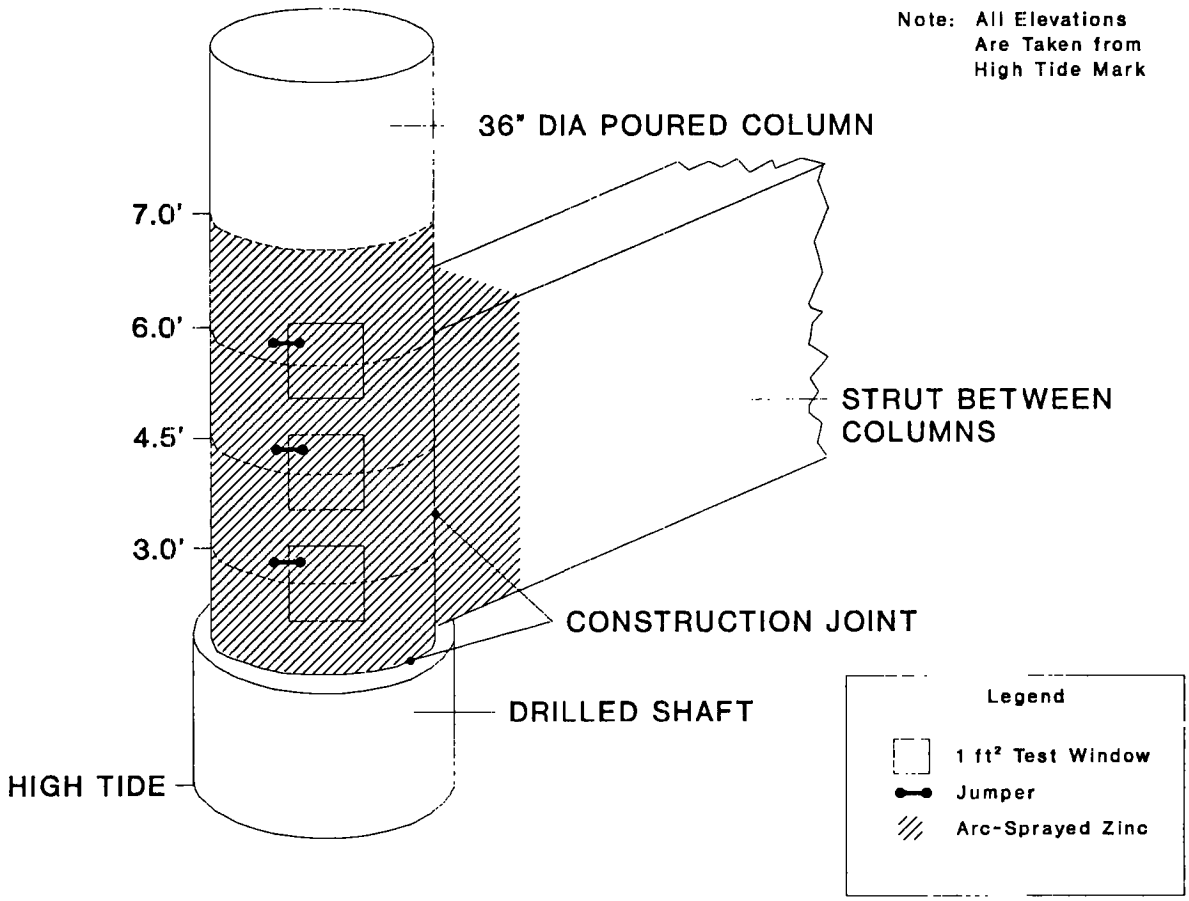

Figure 3.3 Schematic of test site at Niles Channel Bridge (1 in. = 2.54 cm; 1 ft =3 0.5 cm)

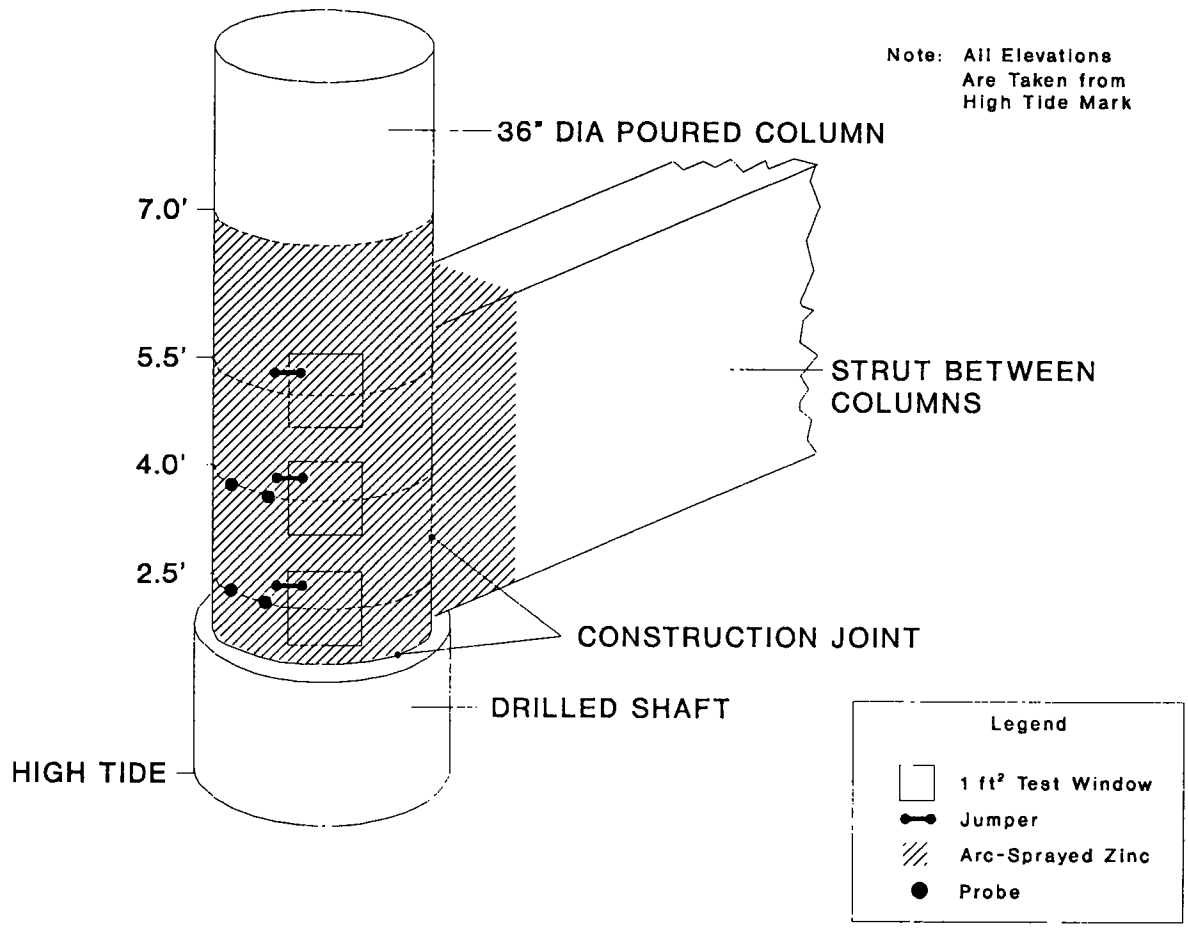

Figure 3.4 Schematic of test site at Seven Mile Bridge (1 in. = 2.54 cm; 1 ft = 30.5 cm)

4

Results—Laboratory Experiments

4.1 Compact Test Specimens

4.1.1 Current Delivery, Galvanic Specimens (No Impressed Current)

Figure 4.1 shows the current delivered by the galvanic specimens (average of each group) with time, for the three humidity exposure conditions used. The currents for all three conditions decreased with time, with the most pronounced decreases at the lowest humidity.

4.1.2 Potentials, Galvanic Specimens

Figures 4.2 through 4.4 show the average instant-off potentials for reinforcing steel and anode in each of the three humidity conditions. In all cases the instant-off potential of the zinc was more negative than that of the reinforcing steel. The difference tended to be greater in the two lower humidity cases. The potentials tended to be nobler at the lower test humidities.

Figure 4.5 shows the average potentials of the normally disconnected control specimens in the high humidity environment. Near the end of the test, the potentials of the control reinforcing steel were slightly less negative than the instant-off values of the steel in the galvanically coupled specimens. The zinc in the controls tended to reach potentials somewhat more negative than the instant-off values measured in the galvanically connected specimens. The final zinc potentials in the disconnected controls were about 200 mV more positive than at the beginning of the test exposure.

4.1.3 Potentials, Impressed-Current Specimens

Maintaining good anode-to-wiring contacts in the impressed-current specimens required constant attention and rebuilding of the contacts during the test. As a result, most of these tests were discontinued after about 300 to 500 days of service, and this report considers only the lower current density tests (1 mA/ft^2 or 1.1 $\mu A/cm^2$), which did not pose severe contact problems.

Figure 4.6 shows the average instant-off potential of the A1-type specimens (single anode slabs, 1 mA/ft^2 [1.1 $\mu A/cm^2$] impressed anode current) at 85% relative humidity as a function of exposure time. The potentials are comparable to those of the galvanic specimens during a comparable test period (see Figures 4.2 and 4.4). This was expected, since the galvanic anodes were initially also delivering current densities on the order of 1 mA/ft^2 (1.1 $\mu A/cm^2$). However, as exposure time increased, the control circuit had to make the anode increasingly more positive to achieve the specified current density.

Figure 4.6 also shows the average trend of the anode instant-off potential (required to achieve 1 mA/ft^2 [1.1 $\mu A/cm^2$]) with time for the A1-type specimens at 25% relative humidity. A dramatic trend toward more positive anode potentials with increasing time was observed. After about 1 year of exposure the power-on potential exceeded several volts. This was consistent with the behavior of the galvanic specimens (Figure 4.1), which unaided delivered only about 0.01 mA/ft^2 (0.011 $\mu A/cm^2$) after about 1 year of service in the low-humidity environment.

Figure 4.7 is the average instant-off potentials for the A3A- and A4A-type specimens at 1 mA/ft^2 (1.1 $\mu A/cm^2$) (bare anode and topcoated anode, respectively). Both the bare and topcoated anodes showed potential trends similar to those of the A1-type specimens, except that the increase in potential requirements as time increased was somewhat more pronounced. The topcoat, applied near day 100, did not have any immediate noticeable effect. The differences observed between uncoated and topcoated material after about 300 days of operation might only reflect the behavior of increasingly unreliable contacts.

Figure 4.8 shows the average potential requirements (to deliver 1 mA/ft^2 [1.1 $\mu A/cm^2$]) for the 85% Zn-15% Al alloy anodes on the A3A- and A4A-type specimens. These anodes had potential requirements typically 200 mV more negative than the commercially pure companion anodes in the same slabs. The organic coating application around day 100 in the A4 specimens created no apparent change in the observed trends.

4.1.4 Resistance

Figure 4.9 shows the average reinforcing steel-to-anode resistance (all galvanic specimens) as a function of exposure time for each of the three environments. While the resistance in the high humidity environment remained relatively constant, the resistance at the other two humidities increased dramatically with time.

The concrete resistivity can be estimated from

$$\rho = (A/d)\ R = 60\ R\ cm$$

where A is the anode or equivalent steel area, d is the bar-anode distance, and R the measured resistance. The ratio A/d is approximately 60 cm for the specimens used. Thus, the nominal concrete resistivity in the 85% relative humidity environment was approximately 6,000–10,000 ohm-cm throughout the test (consistent with typical values for concrete in high humidity conditions).[26]

The resistances between anode and specimen midpoint (where the reference electrode was placed) and steel and midpoint were always roughly half of the values reported in Figure 4.9.

Some anode-lead contact maintenance was required throughout the test to maintain good anode contacts of the galvanic specimens. Before- and after-repair measurements were made periodically to ensure that the resistances were not subject to artifacts from faulty electrode contacts.

4.1.5 Polarization Decay Tests

Figure 4.10 illustrates the behavior observed during the polarization decay tests. These tests were performed on galvanic specimens after 80, 212, and 350 days of testing. Table 4.1 summarizes the average results for all cases. The magnitude of the steel depolarization in the high-humidity environment decreased rapidly with specimen age, becoming less than 10 mV near the end of the first year. The 4-hour steel polarization decay remained near 100 mV after nearly 1 year in the low-humidity environment. Zinc polarization decay remained substantial (about 50 mV after 4 hours) in all conditions throughout the test.

Table 4.1

Steel Polarization Decay Tests, Compact Laboratory Specimens
Average Potential Shift (mV) after 4 and 24 Hours
Following Disconnection

Average Relative Humidity	Exposure Time				
	80 days		212 days		350 days
	4 h	24 h	4 h	24 h	4 h
85%	60	60	14	14	5
60%	110	120	85	95	-
25%	110	130	95	110	90

4.1.6 Polarization Measurements

Figure 4.11 is a typical example of the cathodic behavior of the steel in one of the control specimens at a potential scan rate of 0.05 mV/sec.

Because of the strong mass-transport control and high effective interfacial capacitances encountered with steel in concrete,[27] the polarization behavior was strongly scan-rate dependent. The very low scan rate used approached the practical limit for regular measurements.

There is no clearly defined Tafel-like behavior, so the corrosion rate of the steel could not be estimated. The polarization diagram suggests that cathodic currents on the order of several milliampere (mA) would be needed to shift the potential cathodically by about 100 mV. However, because of the strong scan-rate dependence, the actual current requirement could be much smaller if long-term behavior is considered.

Because of these limitations, most analysis of the system behavior considered only the long-term polarization trends as revealed by the routine current and potential measurements.

Potentiodynamic polarization measurements were also performed in the anodic direction with the sprayed zinc anodes in the control specimens. The same limitations described for the steel apply to those tests, and they will not be addressed further.

4.1.7 Microstructural Examination

Figures 4.12 and 4.13 show metallographic cross sections of the zinc-concrete interface both as deposited and after about 200 days in the high-humidity environment. Porous corrosion products, rich in Zn and Cl, formed on the outer surface of the zinc. Denser reaction products, also rich in Zn and Cl, formed at the porous pockets between successive layers in the zinc deposit and to a lesser extent at the zinc-paste interface. There was no conclusive evidence that an insulating barrier was forming between the anode and the concrete.

4.1.8 Anode Surface Wetting

Specimens from group A0 (three from the 85% and three from the 60% relative humidity environments, simple galvanic operation) were used for these tests, which started at day 330. A damp paper towel was applied to the center of the zinc patch at 0, 48, 96, 144, 240, and 400 hours, and anode-to-midpoint resistance, steel-to-midpoint resistance, instant-off potential, and current delivery were all measured.

Figures 4.14 and 4.15 show the anode-to-midpoint and steel-to-midpoint resistances. Following each wetting, the resistance between the anode and midpoint decreased slightly (the change is too small to be observed in Figure 4.14) and then recovered over a few

hours. The steel-to-midpoint resistance remained virtually unaffected. The sum of the partial resistances was always approximately equal to the measured anode-to-steel resistance.

Figure 4.16 shows the effect of moisture application on the averaged current densities. The specimens in both the 25% and 85% relative humidity environments had a dramatic increase in current immediately upon brief wetting. The current returned to the prewetting values after a few hours.

Figures 4.17 and 4.18 show the effect of wetting on the averaged instant-off potentials. Upon wetting, potentials sharply became more negative. The shifts in potential were typically 250 mV for the anode and 100 mV for the steel at 85% relative humidity, and 200 mV and 100 mV, respectively, at 60% relative humidity. The effect tended to decay during the few hours following wetting.

Polarization decay tests were performed on the specimens immediately before and a few days after the 2-week wetting experiment. The before-and-after results were essentially the same: 90 mV and 5–10 mV decay for the steel in the 60% and 85% environments, respectively (see Table 4.1).

4.2 Instrumented Test Columns

4.2.1 Current Delivery

Figure 4.19 (top) shows the native reinforcing steel current with switches 5 to 8 closed and switch 4 open and the change upon connection to the zinc (switches 1 to 4 closed at day 0). Bar group 5, which was a net anode, ceased net anodic current generation. The other bar groups generally became more cathodic. Note that most of the protective current came from zinc patch 4, closest to the waterline.

The long-term current distribution on the test columns is shown in Figures 4.20 and 4.21. Figure 4.21 shows that, unlike the compact specimens, the total current from the anodes (current at switch 4, Figure 2.3) did not have continuing long-term decay. The current stabilized at a value of about 0.3 mA and was provided by the lowest anode. The upper three anodes contributed negligible current values throughout the test.

Figure 4.22 shows that the fourth set of bars (immediately above the waterline) was the main recipient of the protecting current. The bars in the third set received appreciable current during the first 50 days of exposure and less for the rest of the test. The bars below water (set 5) received very little current throughout.

4.2.2 Potentials

Figure 4.23 shows the average instant-off potentials of the anodes as a function of exposure time. There was an overall trend toward more negative values.

Figure 4.24 shows the average instant-off potentials of the steel bars as a function of time. The behavior followed that of the anodes. The off potential of the bars immediately above and below the waterline were very close throughout the exposure period.

4.2.3 Resistance

Figure 4.25 shows the resistance between each anode and the corresponding bars as a function of time. There was a large increase of resistance with time for the concrete above the waterline. After about 200 days, the resistance of the upper concrete regions was found to be highly dependent on room relative humidity, becoming lower as the relative humidity increased. The resistances from anode to midpoint and steel to midpoint were both roughly equal during early exposure times. At long exposure times in the upper column regions, the resistance between anode and midpoint was greater (often by several times) than that between the steel bars and the midpoint.

4.2.4 Polarization Decay Tests

Table 4.2 summarizes the results of polarization decay tests performed on the test columns after 345, 363, and 650 days of testing. The results show that protection was highest and consistently maintained in the region immediately above the waterline (where corrosion is usually most severe). The differences between the data for days 345 and 363 result partly from the tests shown in the next section.

Table 4.2

4-Hour Polarization Decay Tests, Laboratory Columns
Average Potential Shift (mV)

Bar Level	Exposure Time		
	345 days	363 days	650 days
1	30	60	27
2	60	90	45
3	160	220	127
4	260	310	252
5	-	-	3

4.2.5 Anode Surface Wetting

These tests were performed on the three columns for a 2-week period starting on day 342. The anodes in each column were wetted six times during that period, as described in sections 2.1.7 and 2.2.5.

Figures 4.26 and 4.27 show the anode-to-midpoint and steel-to-midpoint resistances at each of the four anode levels as a function of time. While the steel-to-midpoint values experienced minor variations, the anode-to-midpoint resistances showed dramatic reductions in the chloride-free regions of the columns. The resistances tended to recover relatively slowly. The resistance at the level closest to the water was virtually unaffected by the procedure.

The wetting procedure caused an increase in the amount of current delivery by each anode. Current delivery to the reinforcing steel segments also increased, especially just above the waterline and to a lesser extent just below the waterline. These trends are shown in Figures 4.28 and 4.29.

The current increases were accompanied by a negative shift in potential. The shift was greater in the chloride-free portions of the columns, changing up to 400 mV. This suggests that temporary depassivation of the anode was taking place in the chloride-free regions. The potential decrease at level 4, just above the waterline in high-chloride concrete, was on the order of 100 mV.

Steel depolarization tests were conducted just before and after the end of the wetting experiments. The results, shown in Table 4.2, indicate that the wetting procedures had a longer-lasting effect on the laboratory columns than on the compact specimens.

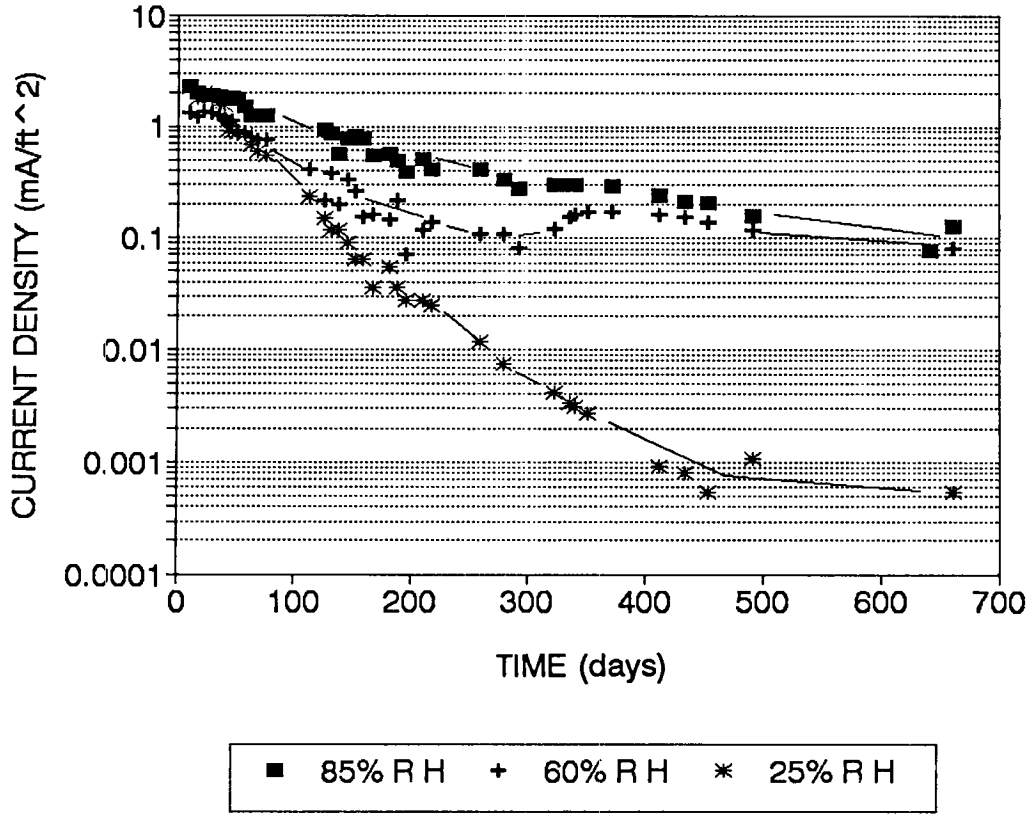

Figure 4.1 **Average current densities of the galvanic test specimens as a function of exposure time for the three relative humidity (RH) environments (1 mA/ft^2 = 1.1 μA/cm^2)**

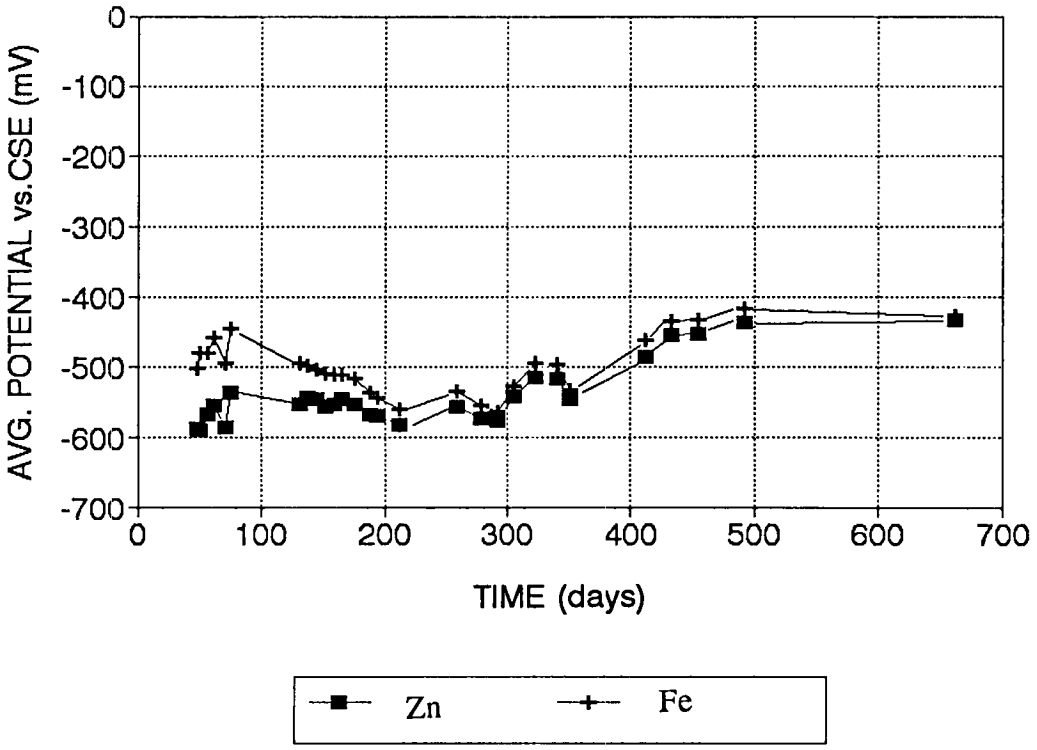

Figure 4.2 **Average instant-off potential of the anode (Zn) and steel (Fe) of the galvanic test specimens in the 85% relative humidity environment as a function of exposure time**

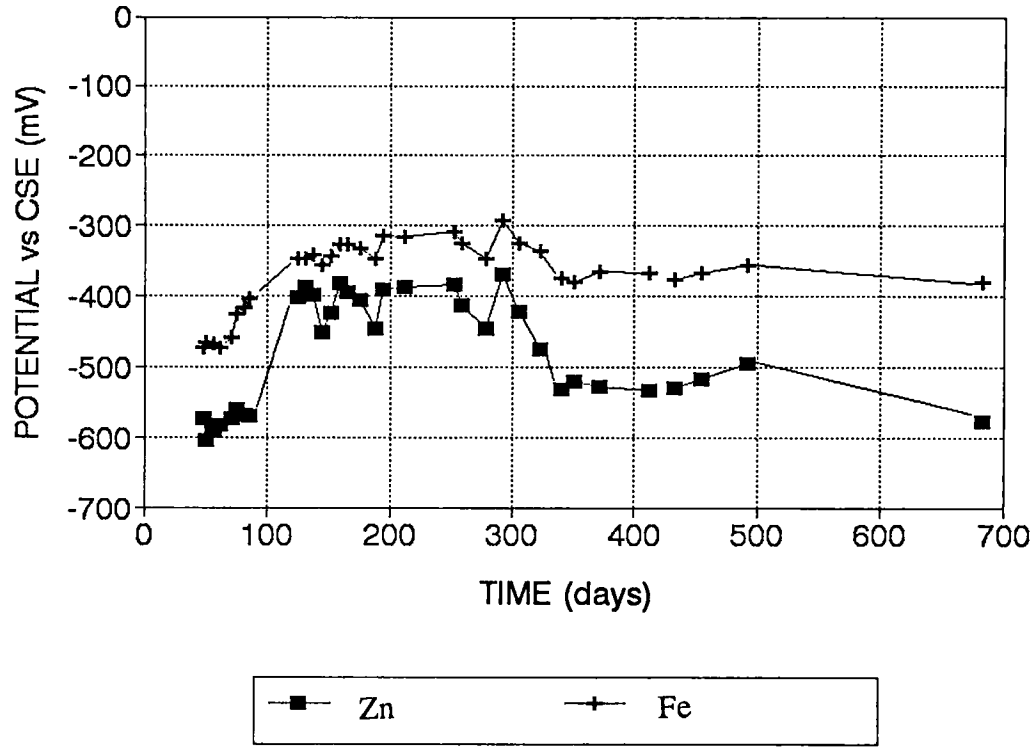

Figure 4.3 **Average instant-off potential of the anode (Zn) and steel (Fe) of the galvanic test specimens in the 60% relative humidity environment as a function of exposure time**

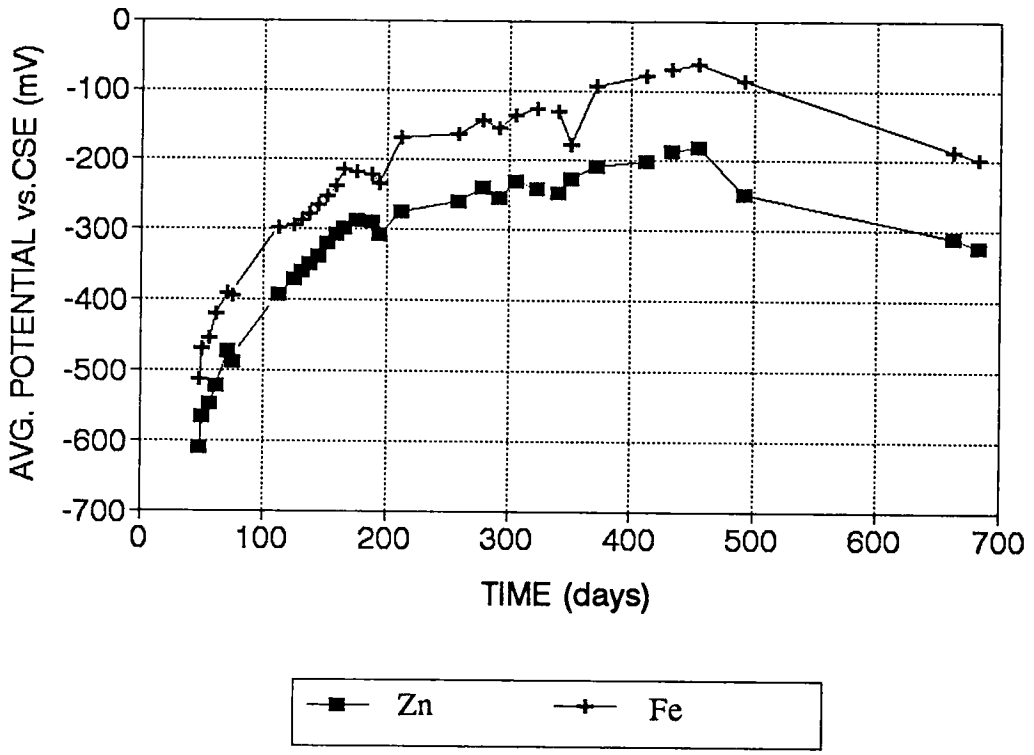

Figure 4.4 **Average instant-off potential of the anode (Zn) and steel (Fe) of the galvanic test specimens in the 25% relative humidity environment as a function of exposure time**

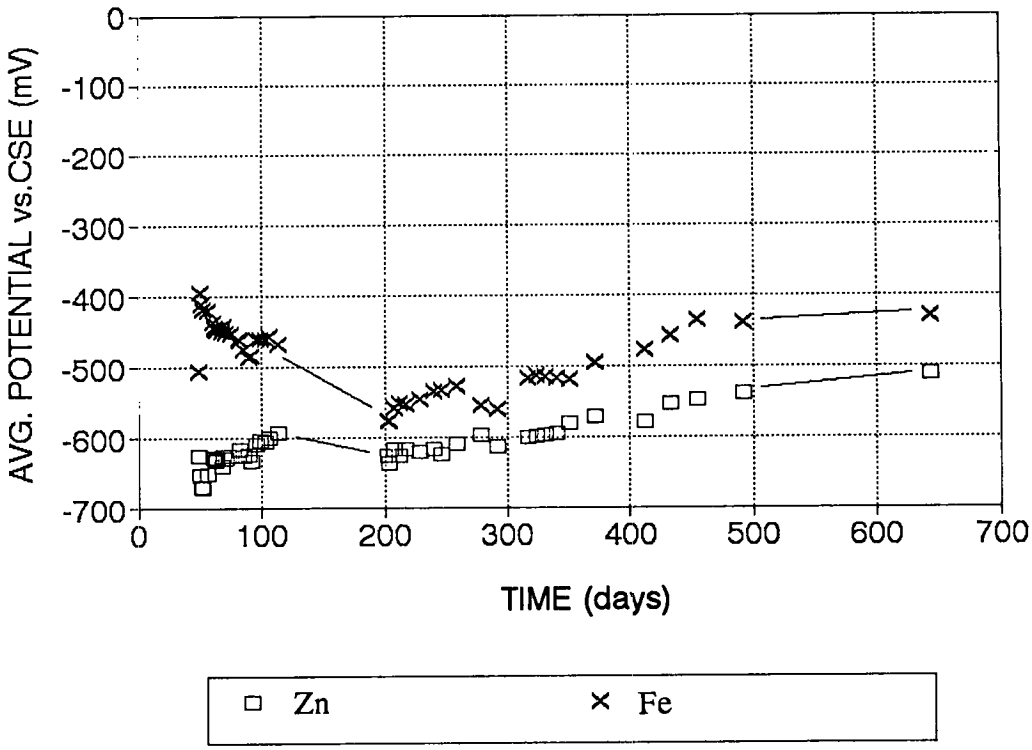

Figure 4.5 **Average potential of the anode (Zn) and steel (Fe) of the control test specimens (always disconnected) in the 85% relative humidity environment as a function of exposure time**

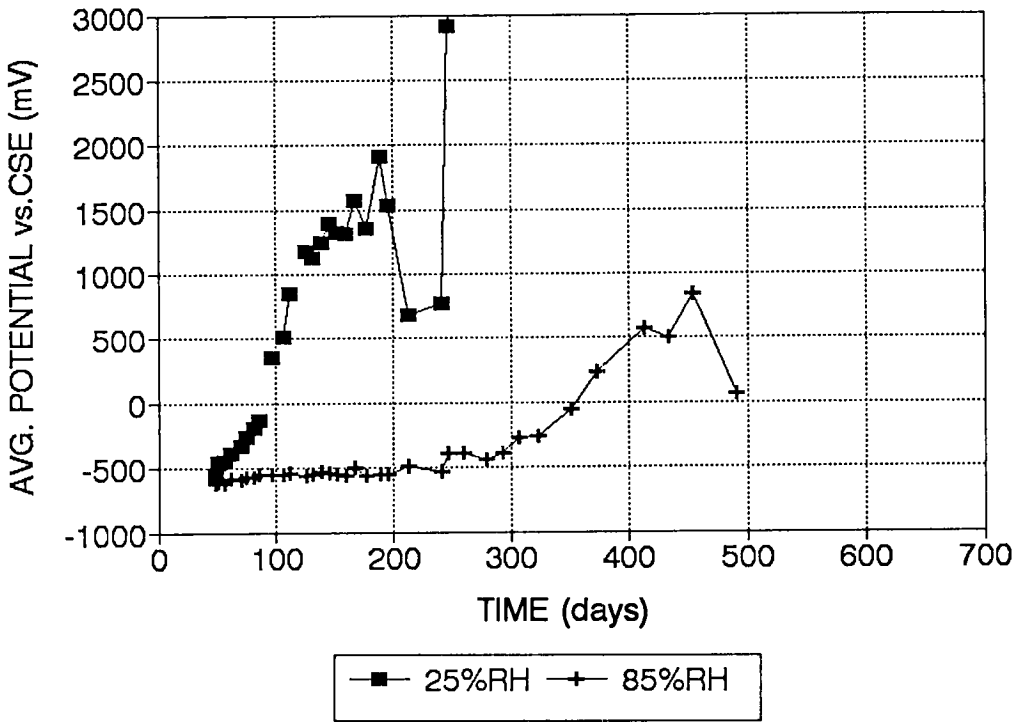

Figure 4.6 **Average instant-off potential of the zinc anode of the 1 mA/ft^2 (1.1 μA/cm^2) impressed-current Type A1 (single anode) test specimens in the 25% and 85% relative humidity (RH) environments as a function of exposure time**

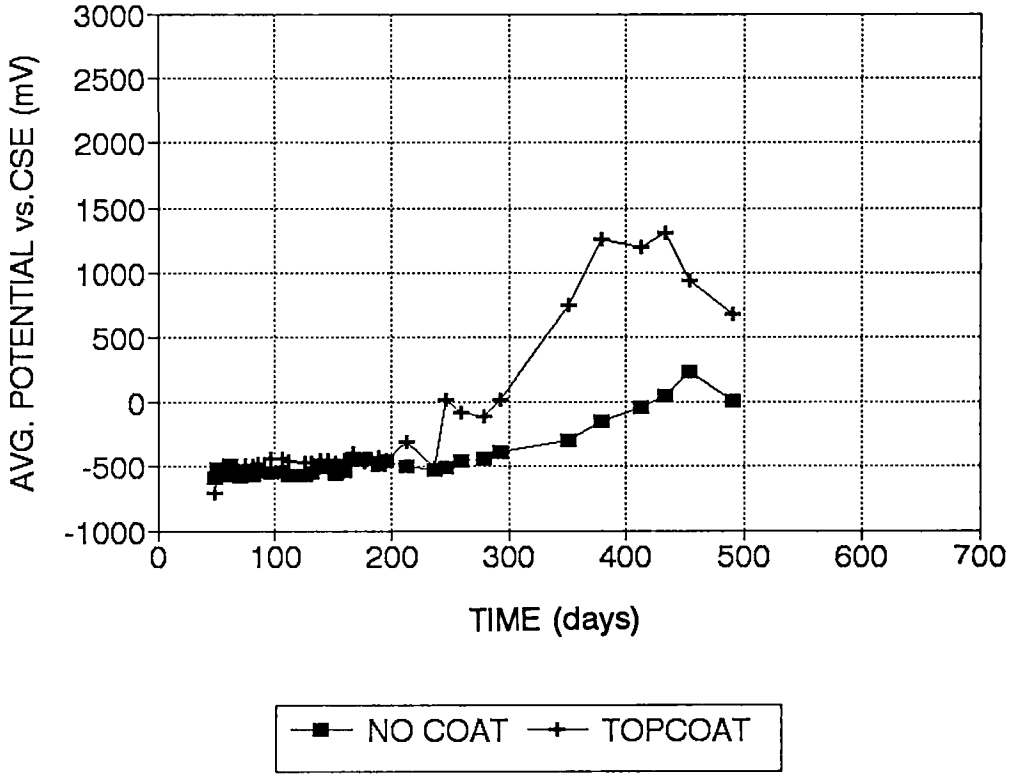

Figure 4.7 **Average instant-off potential of the zinc anode of the 1 mA/ft^2 (1.1 μA/cm^2) impressed-current Type A3 and Type A4 (dual anode uncoated and coated, respectively) test specimens in the 85% relative humidity environment as a function of exposure time**

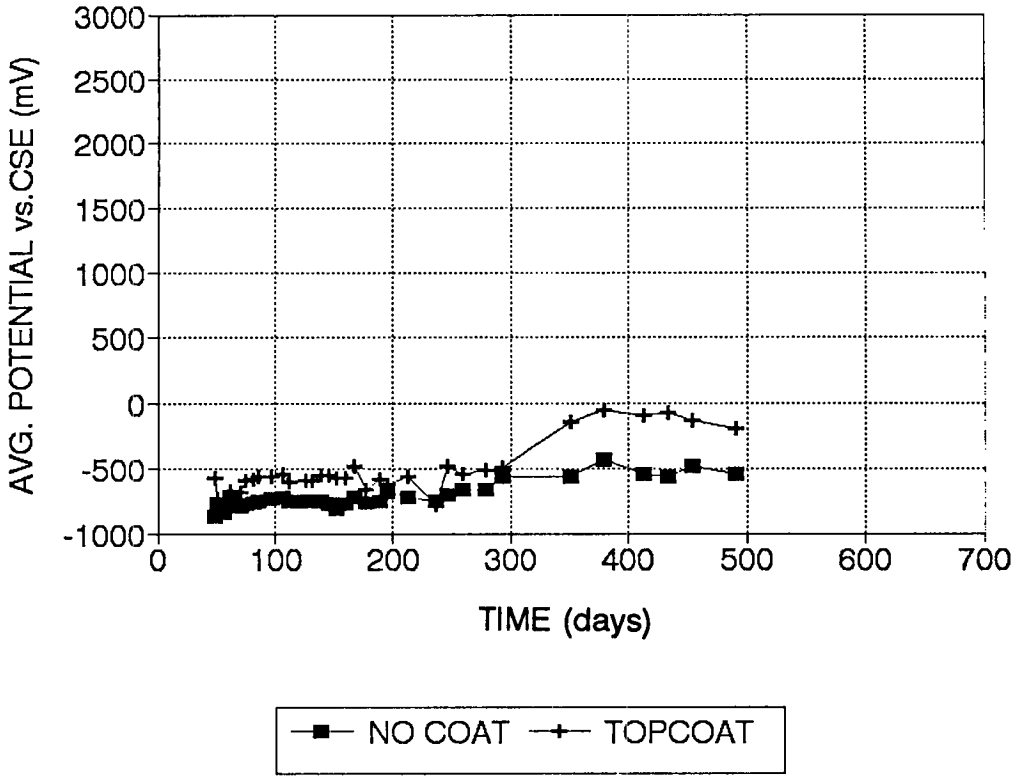

Figure 4.8 **Average instant-off potential of the 85% Zn-15% Al anode of the 1 mA/ft^2 (1.1 μA/cm^2) impressed current Type A3 and Type A4 (dual anode uncoated and coated, respectively) test specimens in the 85% relative humidity environment as a function of exposure time**

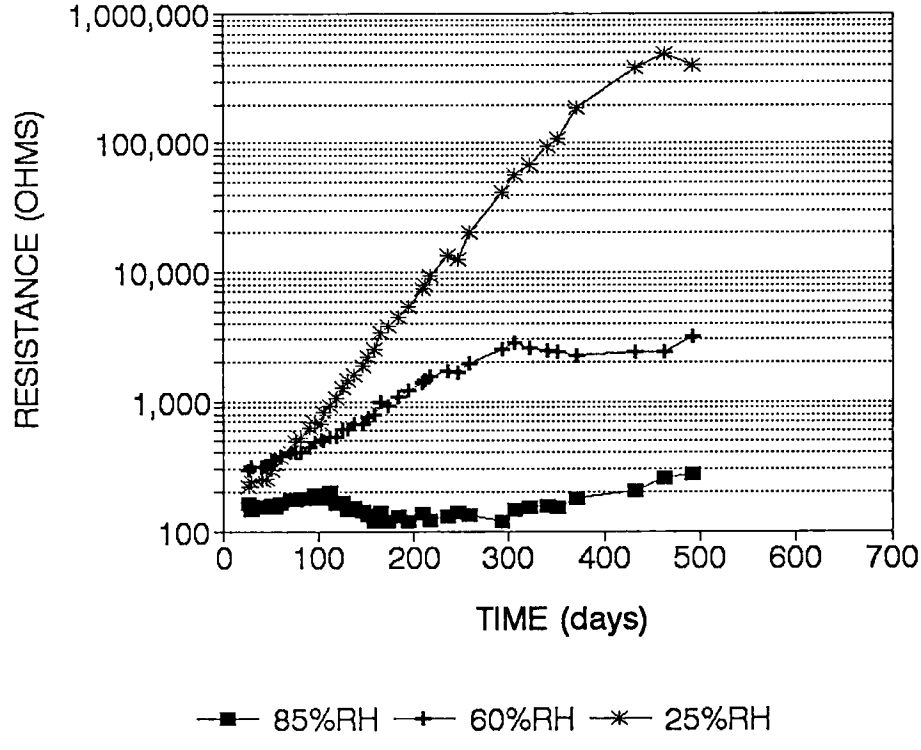

Figure 4.9 **Average anode-to-steel resistance of galvanic specimens in the three relative humidity (RH) environments as a function of exposure time**

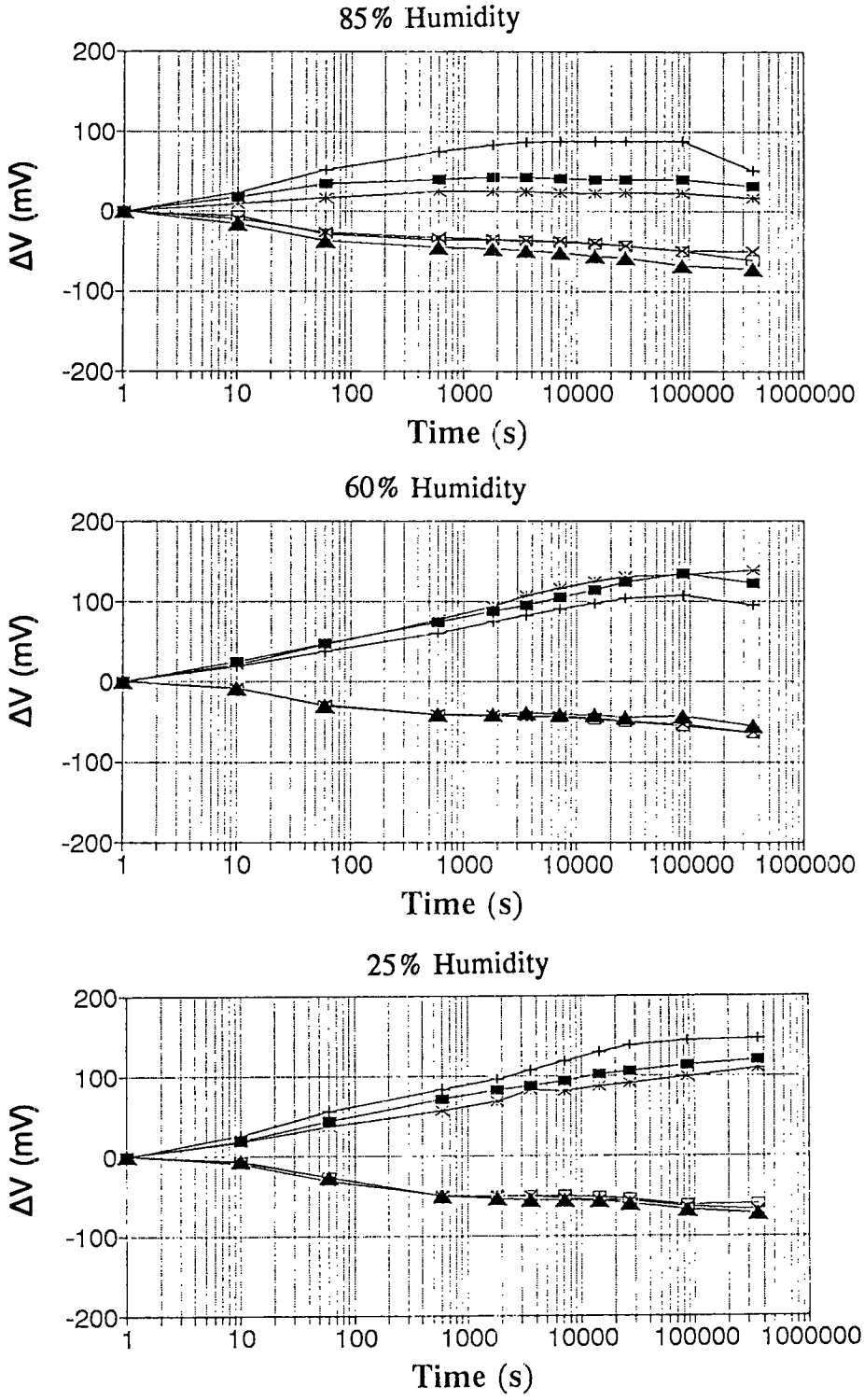

Figure 4.10 **Depolarization test (after 80 days of exposure) of galvanic specimens (test in triplicate). The positive excursions correspond to the rebar; the negative excursions to the zinc anode. All potentials are referenced to the 1-second instant-off value.**

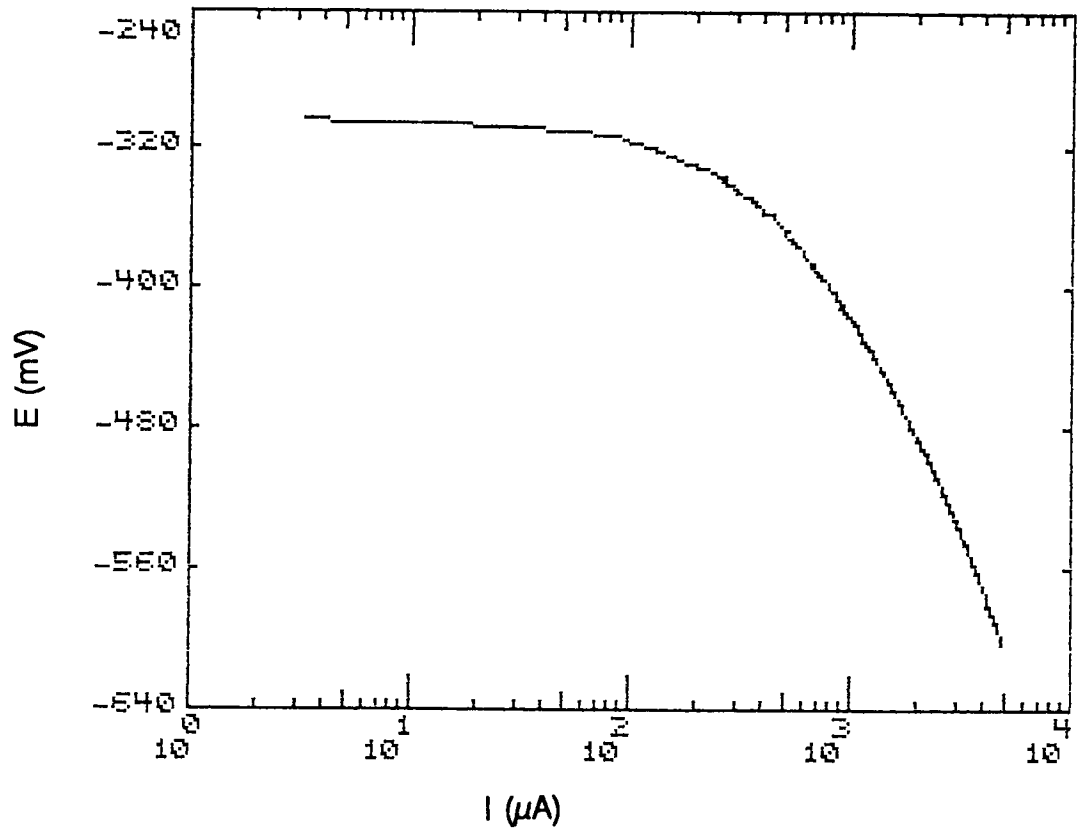

Figure 4.11 **Cathodic polarization test of a control specimen (anode disconnected), performed at 0.05 mV/sec from the open circuit potential in the negative direction. Potentials are versus the internal reference electrode; potentials versus SCE are 170 mV more negative than shown in the plot. Note the lack of well-defined Tafel behavior.**

Figure 4.12 **Typical microstructure of arc-sprayed zinc as revealed in a metallographic cross section. The dark regions and thin lines are porosity resulting from impact and solidification of consecutive droplets on the sprayed surface. Notice how the deposited zinc closely follows the concrete surface. Cement paste and fine aggregates are visible. The coating on this specimen was approximately 250 μm thick. The field shown is 900 μm from top to bottom.**

Figure 4.13 Microstructure of a zinc deposit after approximately 200 days of galvanic service in the 85% relative humidity environment. Porous deposits are present on the outer (top) surface. Zinc corrosion has taken place at the porous pockets between zinc layers and, to a lesser extent, between the zinc and the concrete. The concrete matrix is at bottom. The field shown is 900 μm from top to bottom.

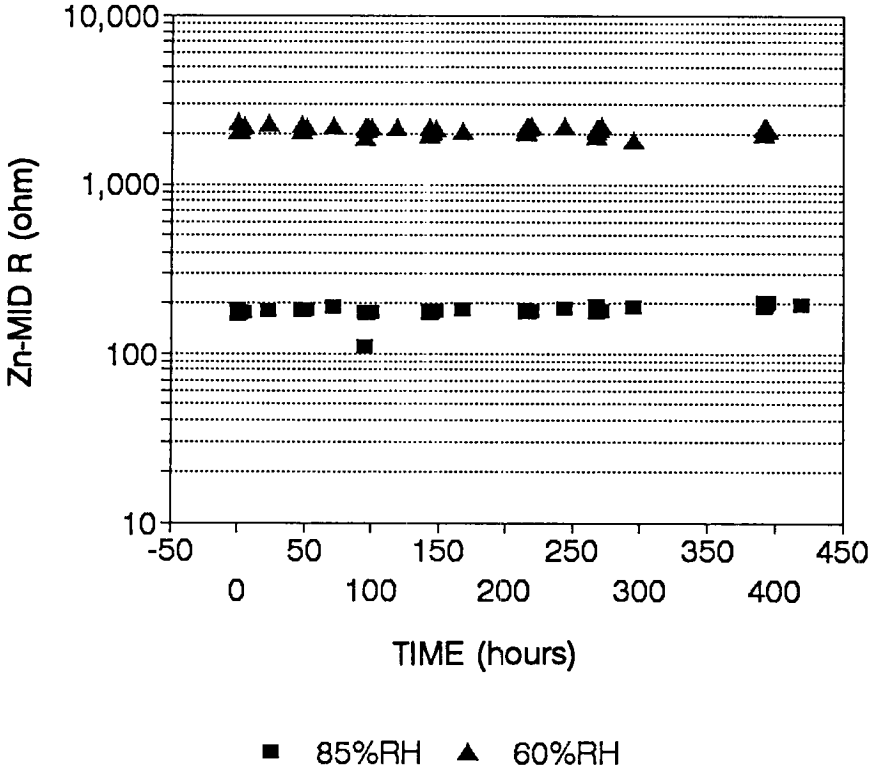

Figure 4.14 Average anode-to-midpoint resistance of galvanic test specimens during the anode wetting sequence as a function of time (RH = relative humidity)

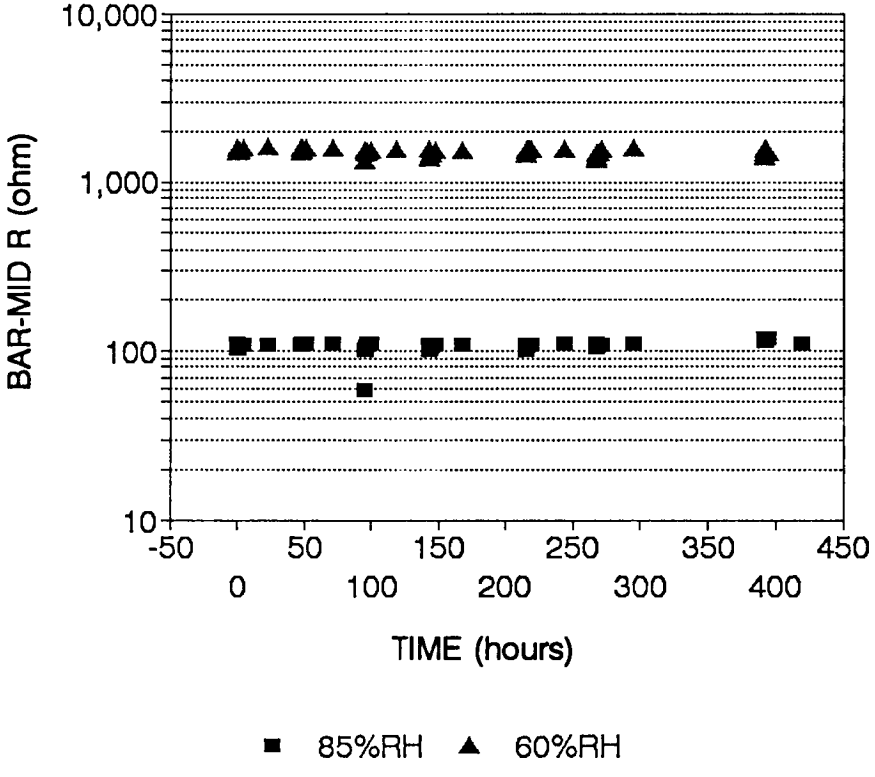

Figure 4.15 Average steel-to-midpoint resistance of galvanic test specimens during the anode wetting sequence as a function of time (RH = relative humidity)

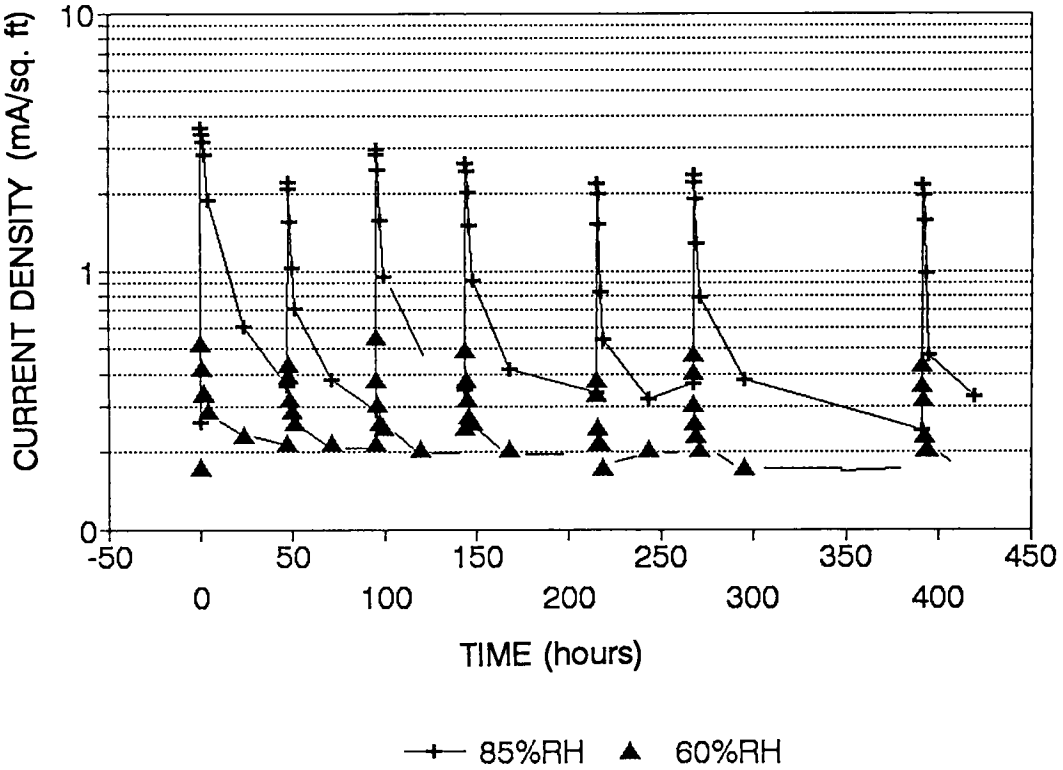

Figure 4.16 **Average anode current density of galvanic test specimens during the anode wetting sequence as a function of time (1 mA/ft^2 = 1.1 μA/cm^2; RH = relative humidity)**

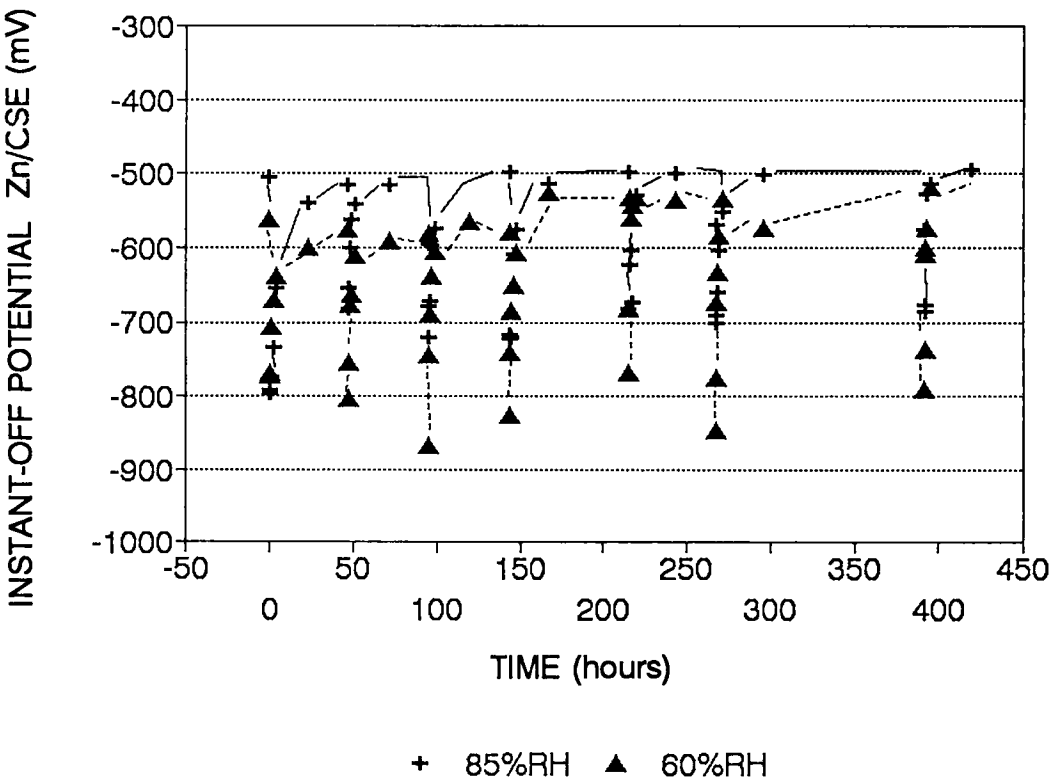

Figure 4.17 **Average anode (Zn) instant-off potential of galvanic test specimens during the anode wetting sequence as a function of time (RH = relative humidity)**

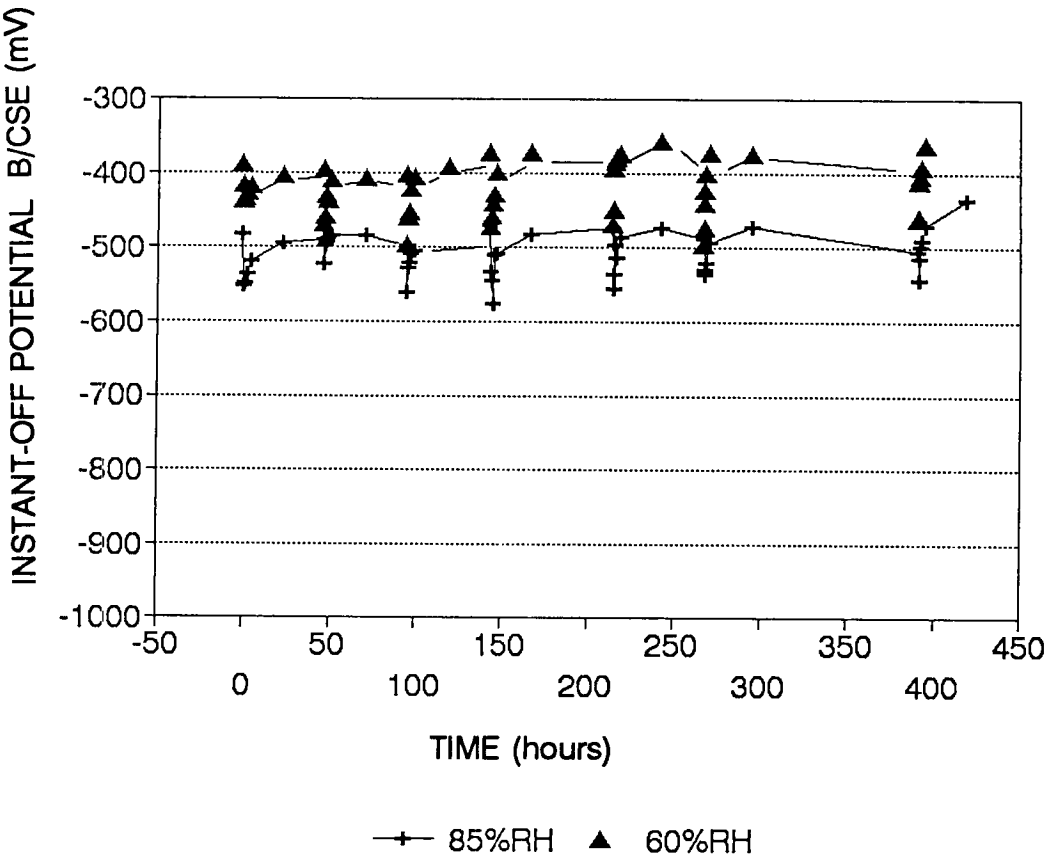

Figure 4.18 **Average steel (B) instant-off potential of galvanic test specimens during the anode wetting sequence as a function of time (RH = relative humidity)**

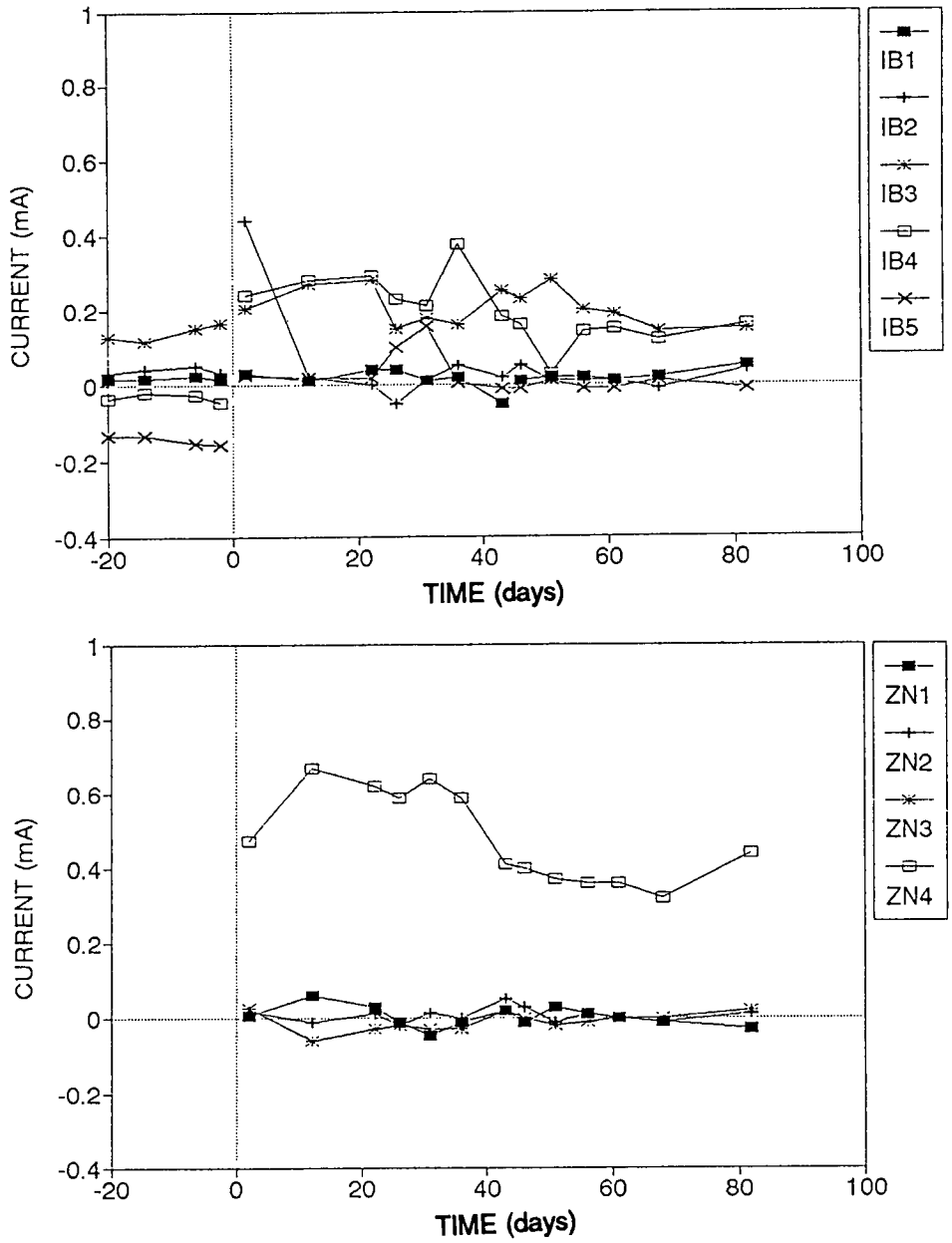

Figure 4.19 **Example of effect (Column A) of anode connection on current distribution patterns. Top: Electronic current consumed or generated at each rebar level, before and after connection of the anodes. Bottom: Corresponding electronic current generated at each anode. See Figure 2.4 for sign convention.**

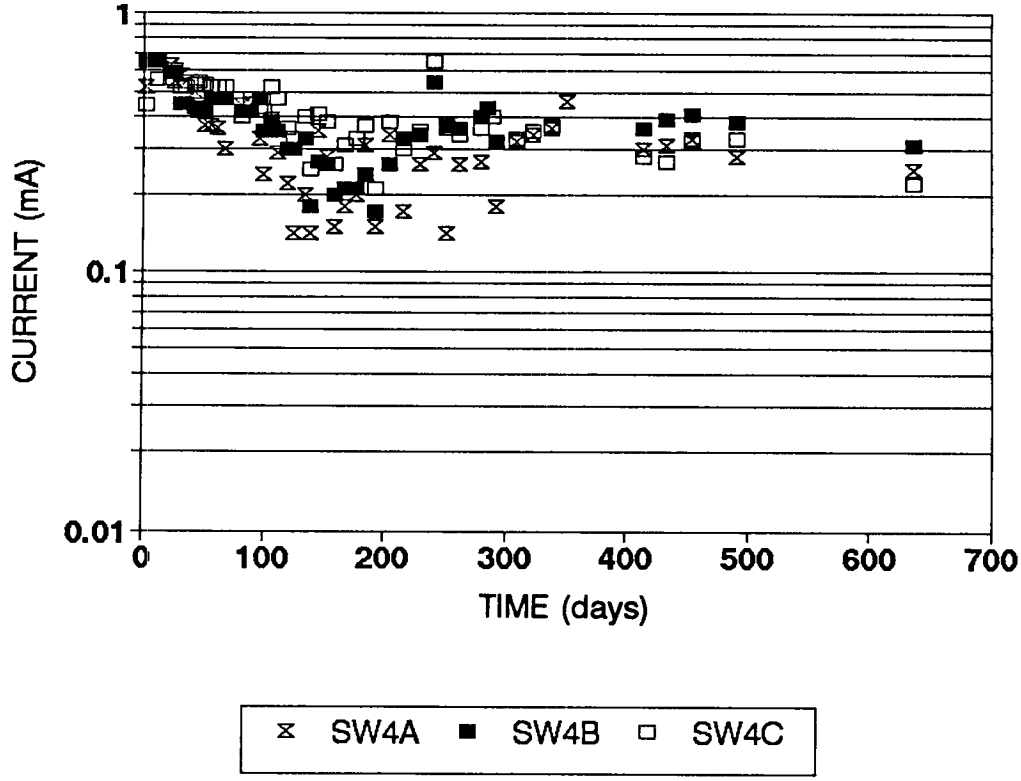

Figure 4.20 Current from all anodes for columns A, B, and C as a function of exposure time

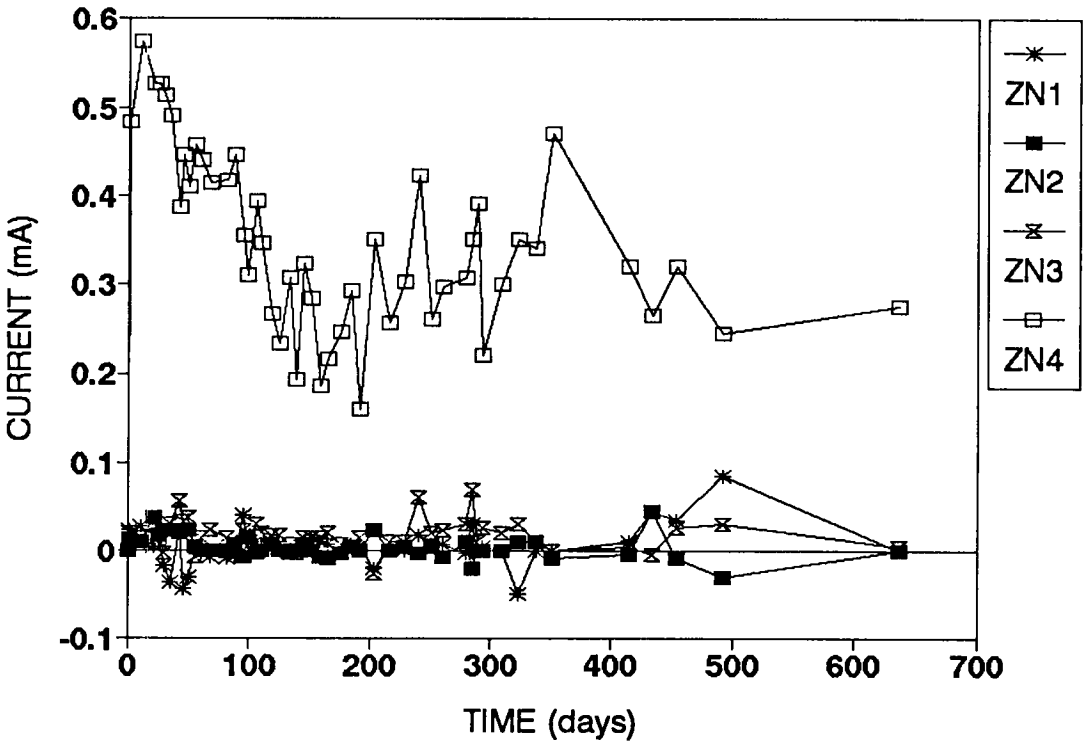

Figure 4.21 Average current from each anode on the laboratory columns as a function of exposure time

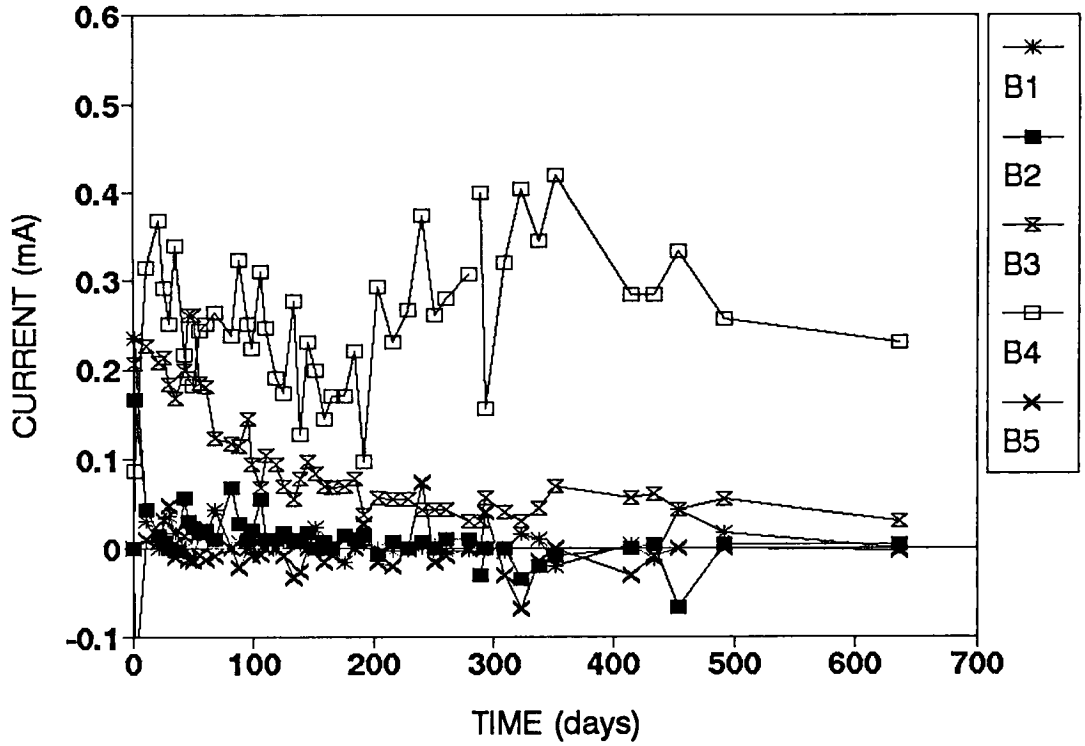

Figure 4.22 Average current to each set of bars on the laboratory columns as a function of exposure time. Bi denotes bar at level i

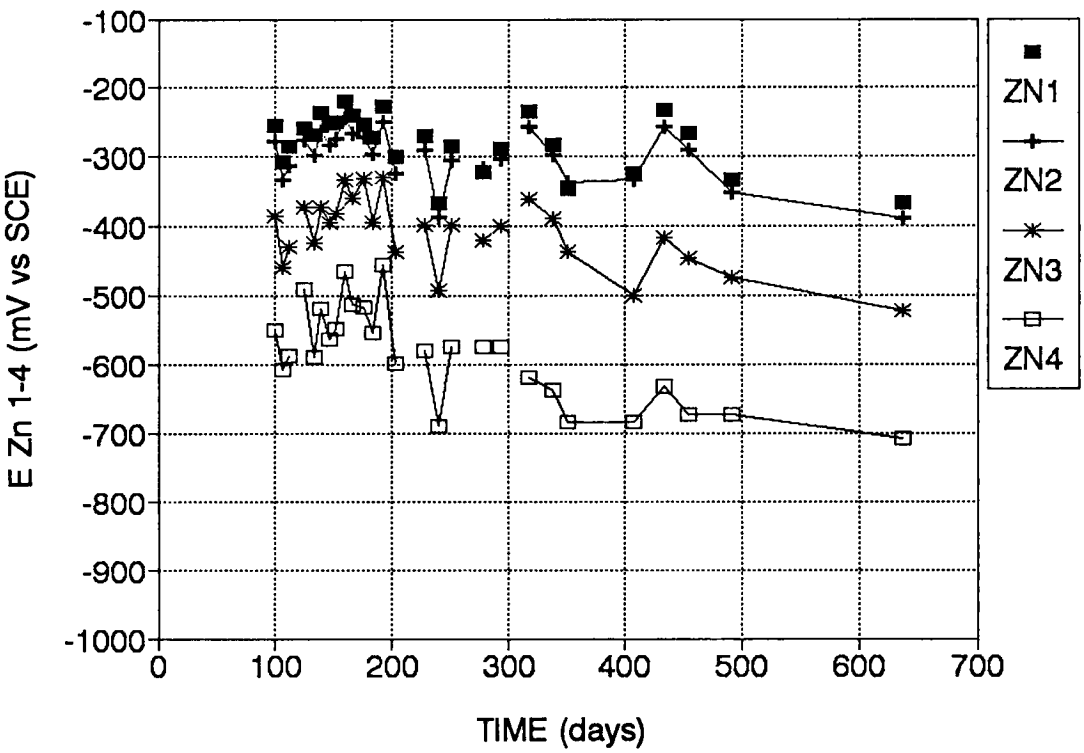

Figure 4.23 Average instant-off potential of each anode as a function of exposure time. These measurements were taken with a saturated calomel electrode (SCE). To convert to potentials versus Cu-$CuSO_4$ subtract 56 mV from the reported SCE values.

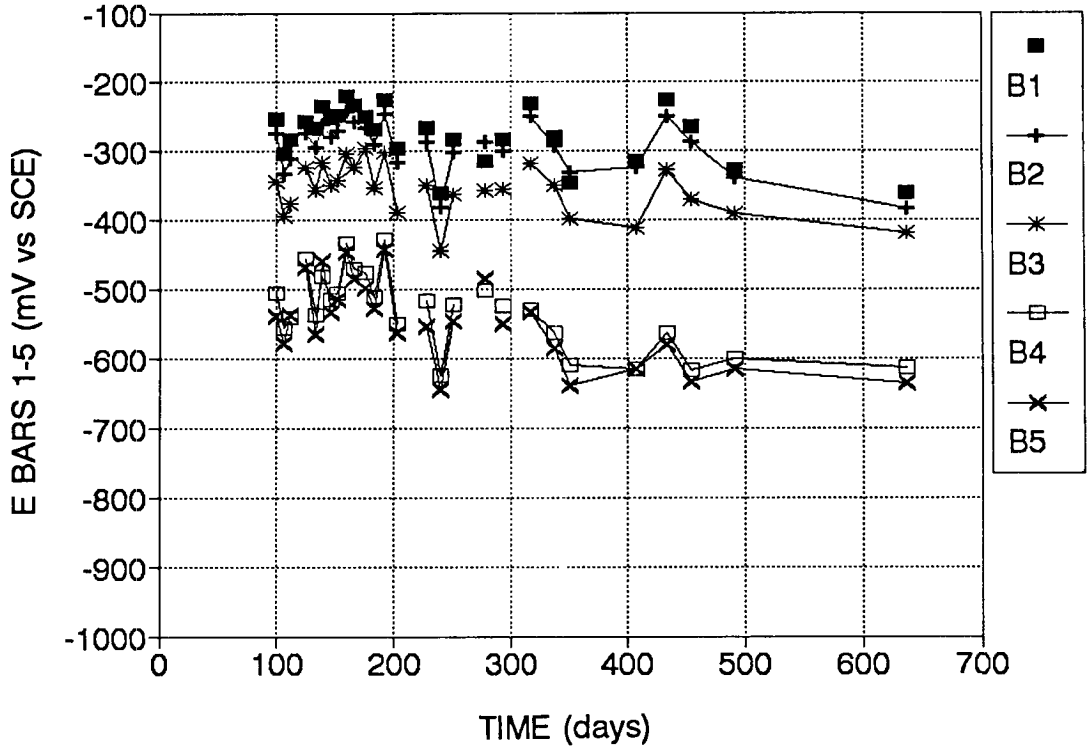

Figure 4.24 **Average instant off potential of each set of bars as a function of exposure time. (These measurements were taken with an SCE; E versus copper sulfate electrode = E versus SCE - 56 mV.)**

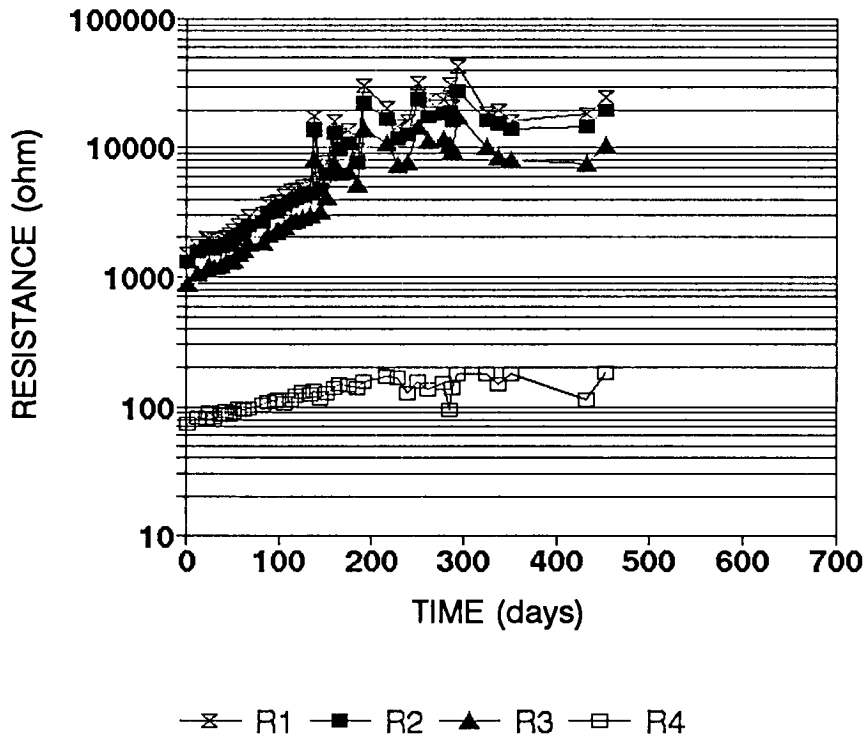

Figure 4.25 **Average resistance between each anode and the corresponding steel bars as a function of exposure time. R1 to R4 correspond to zones 1 to 4, per Figure 2.4.**

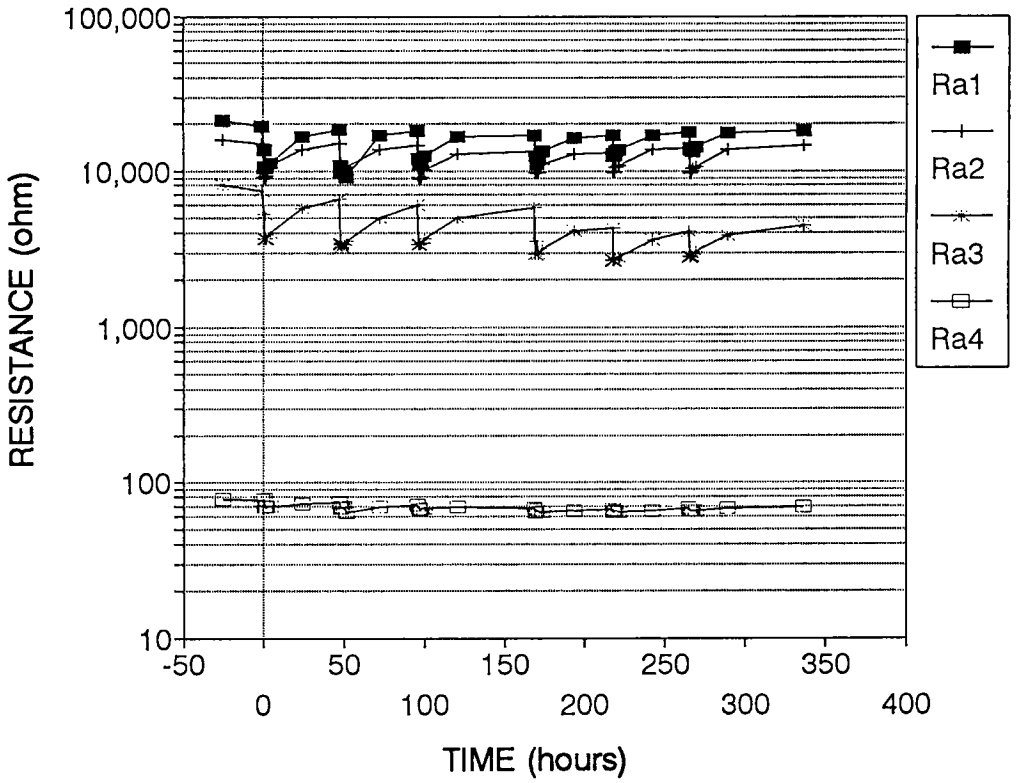

Figure 4.26 **Average resistance, Ra, between the anode and midpoint during the anode wetting sequence as a function of time**

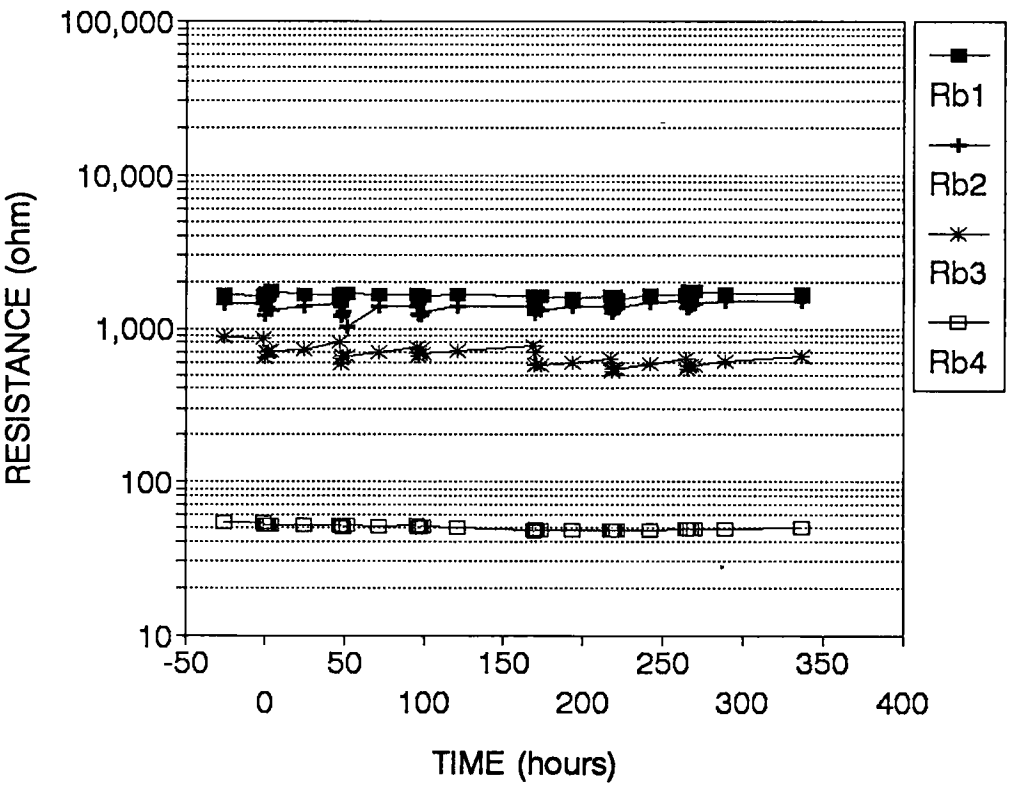

Figure 4.27 **Average resistance Rbi (i denotes level) between steel bars and midpoint at each level of the laboratory columns during the anode wetting sequence as a function of time**

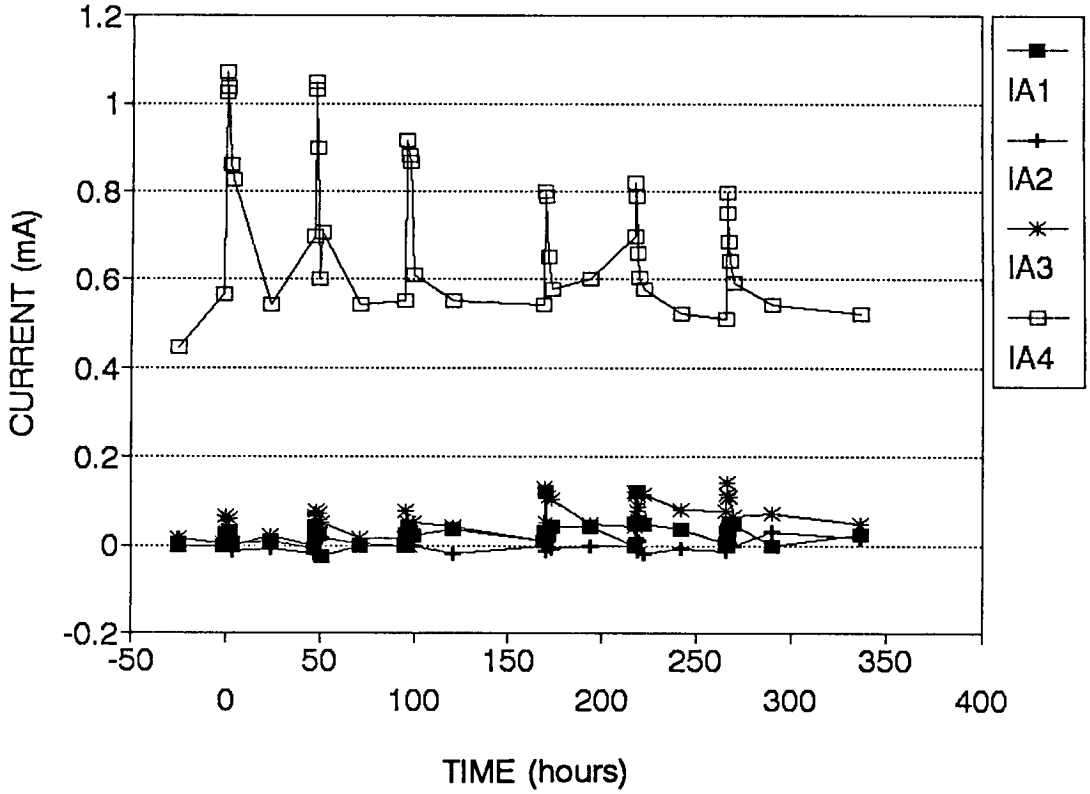

Figure 4.28 Average current IAi (i denotes level) generated by the anodes in response to wetting as a function of time

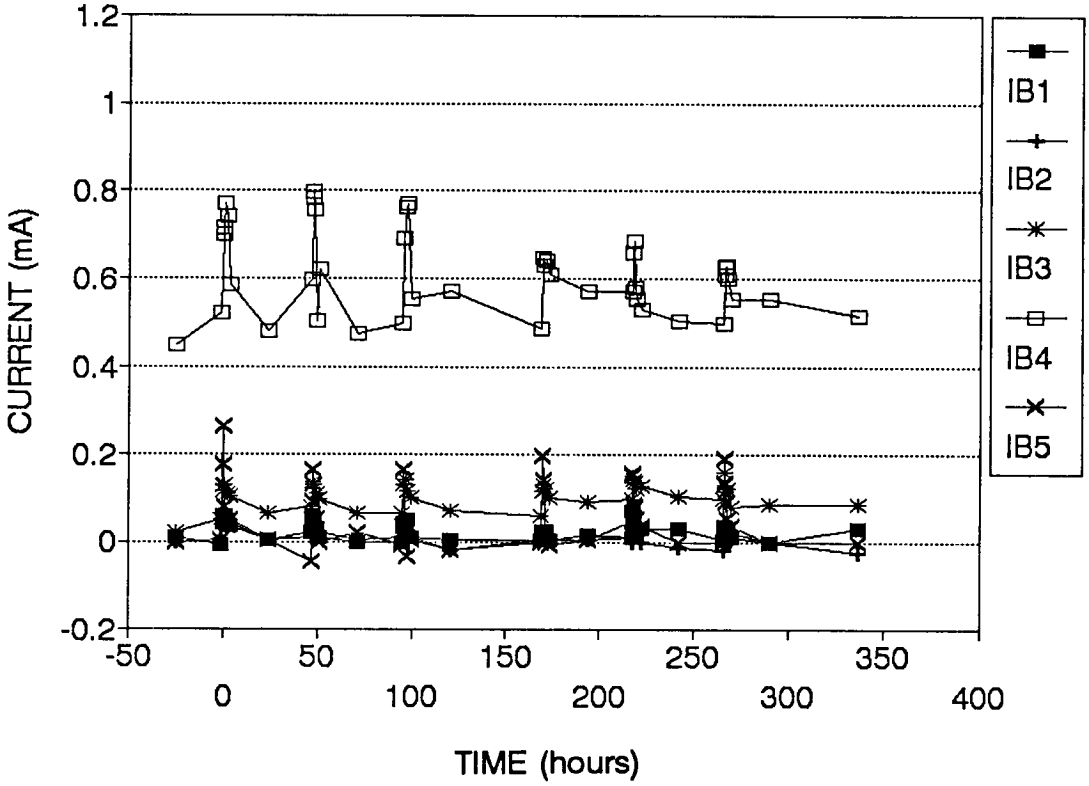

Figure 4.29 Average current IBi (i denotes the level) received by the steel in response to wetting of the anode as a function of time

5

Results—Field Investigations

5.1 Zinc Bond Strength

Bond strength of the sprayed zinc anode was measured with an Elcometer Model 106 fixed-alignment adhesion tester using ASTM D 4541-85 test procedure. Generally, bond strength measurements consisted of three individual tests at locations corresponding to the elevation represented by the zinc windows. In instances where either partial zinc failure or epoxy failure was observed, the test values were not used in the average test value. Results shown in Figure 5.1 are the average of two or three individual tests. Complete tests results are shown in Table 5.1.

5.2 Anode/Cathode Current Density

Current measurements were made using a handheld digital ammeter. Where necessary, current values were computationally corrected to compensate for meter input resistance. Current density of the anode was indirectly evaluated by measuring the current output of the 1 ft^2 (0.093 m^2) windows (see Table 5.2). Current density of the cathode was determined by measuring the current delivery to the embedded reinforcing steel probes. The average anode and cathode currents for each of the test sites are shown in Figures 5.2 through 5.5. For comparative purposes, all anode currents are shown in Figure 5.6.

5.3 Potential Measurements

Anode and cathode half-cell potentials were obtained with a handheld, high-impedance voltmeter set at 200 MΩ. Potential values were measured immediately following current interruption. All half cell-potentials were taken with a copper-copper sulfate reference

electrode. Anode to structure and cathode (bar probe) to anode (zinc) mutual potentials are shown in Table 5.3.

5.4 Window to Structure Resistance

The "window to structure" resistance (Table 5.2) was measured with a Nilsson Model 400 soil resistance meter (97 Hz square wave constant current), configured as a two-point probe. This procedure involved inserting jumpers between the potential and current terminals (see also Figure 2.2) on each side of the meter. One instrument lead was then attached to the window and the other to the surrounding zinc (which is itself electrically continuous with the steel structure). The resistance was then measured after disconnecting the stainless steel jumper band between the window and the zinc/structure.

5.5 Window to Probe Resistance

The resistance between the zinc anode and the embedded reinforcing steel probes was measured using a procedure similar to that described above. Measurements were obtained after connecting the meter leads to the probe and zinc and opening the connection between the probe and zinc. These values are shown in Table 5.3.

5.6 Polarization Decay

Polarization decay of the reinforcing steel probes was measured by interrupting the current and measuring the potential decay (from instant-off) over a period of 1 to 4 hours. These values are shown in Table 5.4 and Figure 5.7. Potential values are with respect to a copper-copper sulfate reference electrode.

Table 5.1 Bond Strength Test

BAHIA HONDA BRIDGE										
DATE	MONTH	ELEV. FT.	TEST A PSI	FAIL %	TEST B PSI	FAIL %	TEST C PSI	FAIL %	AVG. PSI	AVG./ VISIT PSI
04/91	1.4	2.5	150	100	150	100	160	100	153.3	180
04/91	1.4	4	110	100	180	100	180	100	156.6	
04/91	1.4	6	100	100	290	100	130	100	176.3	
04/91	1.4	8	220	100	290	100	200	100	236.6	
10/91	6.9	2.5	100	100					100	170
10/91	6.9	4	150	100					150	
10/91	6.9	6	220	0					220	
10/91	6.9	8	210	100					210	
03/92	12.4	2.5	200	30	100	100			150	170
03/92	12.4	4	---	---					---	
03/92	12.4	6	100	0					100	
03/92	12.4	8	260	0					260	
03/93	23.9	2.5	230	15					230	175
03/93	23.9	4	160	0					160	
03/93	23.9	6	150	20					150	
03/93	23.9	8	160	0					160	
LONG KEY BRIDGE										
04/91	1.4	4.5	50	75	75	100	90	100	78	111.3
04/91	1.4	6	280	100	110	100	130	100	144	
04/91	1.4	7.5	180	100	100	0	180	100	112	
10/91	6.9	4.5	120	100					120	120
10/91	6.9	6	120	100					120	
10/91	6.9	7.5	120	100					120	
03/92	12.4	4.5	100	100					100	123.3
03/92	12.4	6	140	100					140	
03/92	12.4	7.5	130	100					130	
03/93	23.9	4.5	70	60					70	103.3
03/93	23.9	6	140	100					140	
03/93	23.9	7.5	100	100					100	

Table 5.1 (Continued)

NILES CHANNEL BRIDGE										
DATE	MONTH	ELEV. FT.	TEST A PSI	FAIL %	TEST B PSI	FAIL %	TEST C PSI	FAIL %	AVG. PSI	AVG./ VISIT PSI
04/91	30.3	3	300	100	200	100	150	90	216.6	315.5
04/91	30.3	4.5	210	0	280	0	340	30	276.6	
04/91	30.3	6	620	0	490	0	250	20	453.3	
10/91	35.9	3	150	100					150	215
10/91	35.9	4.5	280	100					280	
10/91	35.9	6	—	—					—	
03/92	41.4	3	200	0					200	171.6
03/92	41.4	4.5	190	0					190	
03/92	41.4	6	125	0					125	
SEVEN MILE BRIDGE										
04/91	1.4	2.5	90	100	120	100	100	100	103.3	123.3
04/91	1.4	4	140	100	190	100	100	80	14.3	
10/91	6.9	2.5	125	100					125	112.5
10/91	6.9	4	100	0					100	
03/92	12.4	2.5	—	—					—	
03/92	12.4	4	—	—					—	
03/93	23.9	2.5	90	0					100	120
03/93	23.9	4	180	100					140	

Table 5.2 Window to Structure Electrical Properties

BAHIA HONDA BRIDGE						
Date	Months	Elev. FT.	V (mV)	Res (Ohm)	Current (mA/Ft^2)	Average (mA/Ft^2)
04/16/91	1.4	2.5	135	22	1.99	1.886
04/16/91	1.4	4	203	23	3.02	
04/16/91	1.4	6	184	63	1.42	
04/16/91	1.4	8	240	100	1.11	
10/03/91	6.9	2.5	102	23	0.57	0.788
10/03/91	6.9	4	185	46	1.18	
10/03/91	6.9	6	167	77	0.73	
10/03/91	6.9	8	221	140	0.66	
03/17.92	12.4	2.5	82	22	3.99	2.903
03/17/92	12.4	4	173	43.5	3.91	
03/17/92	12.4	6	165	73.5	2.17	
03/17/92	12.4	8	197	120	1.53	
03/03/93	23.9	2.5	91	21	2.97	1.598
03/03/93	23.9	4	117	41	1.54	
03/03/93	23.9	6	112	70	1.05	
03/03/93	23.9	8	138	100	0.83	
04/29/93	25.8	2.5	134	220	0.51	0.408
04/29/93	25.8	4	26	43	0.45	
04/29/93	25.8	6	36	78	0.34	
04/29/93	25.8	8	23	130	0.26	
LONG KEY BRIDGE						
04/18/91	1.4	4.5	78	65	0.93	0.548
04/18/91	1.4	6	47	72	0.51	
04/18/91	1.4	7.5	28	91	0.20	
10/03/91	6.9	4.5	28	70.5	0.33	0.436
10/03/91	6.9	6	30	76	0.81	
10/03/91	6.9	7.5	12	95.5	0.16	
03/17/92	12.4	4.5	11	76	0.11	0.175
03/17/92	12.4	6	29	80	0.27	
03/17/92	12.4	7.5	18	100	0.14	
03/03/93	23.9	4.5	12	100	0.26	0.295
03/03/93	23.9	6	1	80	0.06	
03/03/93	23.9	7.5	31	101	0.56	

Table 5.2 (Continued)

NILES CHANNEL BRIDGE						
Date	Months	Elev. FT.	V (mV)	Res (Ohm)	Current (mA/Ft^2)	Average (mA/Ft^2)
04/19/91	30.4	3	56	110	0.39	0.535
04/19/91	30.4	4.5	54	83	0.61	
04/19/91	30.4	6	63	100	0.61	
10/03/91	35.9	3	140	195	0.02	0.078
10/03/91	35.9	4.5	80	91.5	0.12	
10/03/91	35.9	6	21	115	0.09	
03/17/92	41.4	3	34	280	0.33	0.352
03/17/92	41.4	4.5	5	100	0.23	
03/17/92	41.4	6	15	130	0.49	
03/03/93	52.9	3	5	700	0.02	0.643
03/03/93	52.9	4.5	42	150	1.04	
03/03/93	52.9	6	16	200	0.87	
04/29/93	54.8	3	41	210	0.12	0.261
04/29/93	54.8	4.5	40	110	0.37	
04/29/93	54.8	6	29	120	0.30	
SEVEN MILE BRIDGE						
04/19/91	1.4	2.5	31	59	0.41	0.471
04/19/91	1.4	4	47	760	0.40	
04/19/91	1.4	5	60	110	0.61	
10/03/91	6.9	2.5	90	59	1.53	0.896
10/03/91	6.9	4	85	340	0.30	
10/03/91	6.9	5	99	110	0.86	
03/17/92	12.4	2.5	138	88	0.95	0.665
03/17/92	12.4	4	158	120	0.69	
03/17/92	12.4	5	97	230	0.35	
03/03/93	23.9	2.5	72	110	0.50	0.399
03/03/93	23.9	4	106	140	0.46	
03/03/93	23.6	5	84	240	0.22	
04/29/93	25.8	2.5	30	107	0.21	0.208
04/29/93	25.8	4	36	120	0.21	
04/29/93	25.8	5	66	250	0.23	

Table 5.3 Probe (Cathode) Current

BAHIA HONDA BRIDGE								
Date	Months Between Readings	Elev. Ft.	V (mV)	Res. (ohm)	Current (mA)	Curr. mA/Ft^2	Avg. I mA/Ft^2 /Visit	Avg. I mA/Ft^2 /Elev.
04/16/91	0.4	2.5	382	460	—	—	3.14	0.331
04/16/91	0.4	4	156	1200	0.05	3.628		2.454
04/16/91	0.4	6	239	1000	0.04	2.908		1.868
04/16/91	0.4	8	255	1900	0.05	2.89		1.039
10/03/91	5.5	2.5	333	460	—	—		
10/03/91	5.5	4	162	1200	0.39	2.87	1.81	
10/03/91	5.5	6	82	1000	0.02	1.483		
10/03/91	5.5	8	35	1900	0.01	1.094		
03/17/92	5.4	2.5	99	2700	0.005	0.331		
03/17/92	5.4	4	144	1400	0.019	1.382	0.824	
03/17/92	5.4	6	162	1300	0.020	1.425		
03/17/92	5.4	8	109	2500	0.002	0.158		
03/03/93	11.5	4	173	1200	0.033	2.354	1.341	
03/03/93	11.5	6	151	1500	0.023	1.65		
03/03/93	11.5	8	65	1300	0.0002	0.014		
LONG KEY BRIDGE								
04/18/91	0	4.5	—	—	—	—	—	—
04/18/91	0	6	—	—	—	—	—	—
04/18/91	0	7.5	—	—	—	—	—	—
10/03/91	5.5	4.5	383	55	0.102	7.308	7.308	5.1264
10/03/91	5.5	6	—	—	—	—	—	4.7844
10/03/91	5.5	7.5	—	—	—	—	—	1.9908
03/17/92	5.4	4.5	262	950	0.066	4.780	4.421	
03/17/92	5.4	6	243	720	0.072	5.162		
03/17/92	5.4	7.5	248	720	0.046	3.319		
03/03/93	11.5	4.5	381	860	0.046	3.290	2.786	
03/03/93	11.5	6	435	790	0.061	4.406		
03/03/93	11.5	7.5	483	1020	0.009	0.6624		

Table 5.3 (Continued)

NILES CHANNEL BRIDGE								
Date	Months Between Readings	Elev. Ft.	V (Mv)	Res (Ohm)	Current (mA)	Curr. mA/Ft^2	Avg. I mA/Ft^2 /Visit	Avg. I mA/Ft^2 /Elev.
04/19/91	10	5	—	—	0.004	0.273	0.378	0.1638
04/19/91	10	4	—	—	0.006	0.463		0.2988
04/19/91	10	3	—	—	0.007	0.528		0.4878
04/19/91	10	2	—	—	0.004	0.253		0.459
10/03/91	5.5	5	—	—	0.002	0.144	0.283	
10/03/91	5.5	4	—	—	0.004	0.274		
10/03/91	5.5	3	—	—	0.006	0.401		
10/03/91	5.5	2	—	—	0.004	0.313		
03/17/92	5.4	5	—	—	0.001	0.078	0.128	
03/17/92	5.4	4	—	—	0.003	0.188		
03/17/92	5.4	3	—	—	0.003	0.211		
03/17/92	5.4	2	—	—	0.001	0.034		
03/03/93	11.5	5	—	—	0.002	0.144	0.623	
03/03/93	11.5	4	—	—	0.004	0.288		
03/03/93	11.5	3	—	—	0.012	0.817		
03/03/93	11.5	2	—	—	0.017	1.244		
SEVEN MILE BRIDGE								
04/19/91	0.4	2.5	291	830	0.093	6.934	7.999	5.1156
04/19/91	0.4	4	326	690	0.169	9.065		6.0426
10/03/91	5.5	2.5	113	900	0.123	8.662	10.616	
10/03/91	5.5	4	150	845	0.175	12.572		
03/17/92	5.4	2.5	139	970	0.048	3.434	2.199	
03/17/92	5.4	4	111	1000	0.013	0.958		
03/03/93	11.5	2.5	504	1700	0.020	1.438	1.501	
03/03/93	11.5	4	302	1900	0.022	1.570		

Table 5.4 Probe Depolarization Test

BAHIA HONDA BRIDGE							
TIME ON (Months)	ELEV. (ft)	CURRENT (mA/Ft^2)	POT. ON (-mV)	INST OFF (-mV)	FINAL POT. (-mV)	TOTAL DECAY (mV)	AVG. DECAY/ VISIT (mV)
1.4	2.5	14.43	654	630	327	303	169
1.4	4	3.63	573	517	463	54	
1.4	6	2.91	563	526	387	139	
1.4	8	2.89	530	503	323	180	
6.9	2.5	20.56	831	759	381	378	170
6.9	4	2.88	593	503	391	112	
6.9	6	1.48	454	432	335	97	
6.9	8	1.10	302	296	203	93	
12.4	2.5	0.33	483	463	379	84	101.5
12.4	4	1.38	425	397	299	98	
12.4	6	1.43	389	380	243	137	
12.4	8	0.16	265	262	175	87	
23.9	2.5	N/A	565	553	324	229	144.8
23.9	4	2.35	463	442	303	139	
23.9	6	1.66	418	400	282	118	
23.9	8	0.01	307	301	208	93	
LONG KEY BRIDGE							
1.4	4.5	N/A	N/A	N/A	N/A	0	0
1.4	6	N/A	N/A	N/A	N/A	0	
1.4	7.5	N/A	N/A	N/A	N/A	0	
6.9	4.5	7.31	725	689	535	154	154
6.9	6	N/A	N/A	N/A	N/A	0	
6.9	7.5	N/A	N/A	N/A	N/A	0	
12.4	4.5	4.78	603	492	338	154	195
12.4	6	5.16	628	616	387	229	
12.4	7.5	3.32	582	547	345	202	
23.9	4.5	3.29	541	534	416	118	125.5
23.9	6	4.41	553	521	367	154	
23.9	7.5	0.66	406	395	298	97	

Table 5.4 (Continued)

NILES CHANNEL BRIDGE							
TIME ON (Months)	ELEV. (ft)	CURRENT (mA/Ft^2)	POT. ON (-mV)	INST OFF (-mV)	FINAL POT. (-mV)	TOTAL DECAY (mV)	AVG. DECAY/ VISIT (mV)
1.4	5	.273	611	610	486	124	118
1.4	4	.465	750	731	596	135	
1.4	3	.528	477	471	362	109	
1.4	2	.253	458	456	352	104	
6.9	5	.143	198	216	116	100	111.8
6.9	4	.274	294	286	191	95	
6.9	3	.401	339	323	207	116	
6.9	2	.313	407	399	263	136	
12.4	5	.078	296	295	219	76	77.5
12.4	4	.188	320	317	225	92	
12.4	3	.211	346	338	237	101	
12.4	2	.034	263	259	218	41	
23.9	5	.162	226	218	120	98	143
23.9	4	.279	308	252	178	74	
23.9	3	.817	357	332	135	197	
23.9	2	1.244	451	432	229	203	
SEVEN MILE BRIDGE							
1.4	2.5	6.93	693	617	406	211	218.5
1.4	4	9.07	670	601	375	226	
6.9	2.5	8.66	533	525	428	97	84
6.9	4	12.57	436	396	325	71	
12.4	2.5	3.43	487	463	329	134	131.5
12.4	4	0.96	432	425	296	129	
23.9	2.5	1.43	476	474	43	431	353.5
23.9	4	1.57	410	405	129	276	

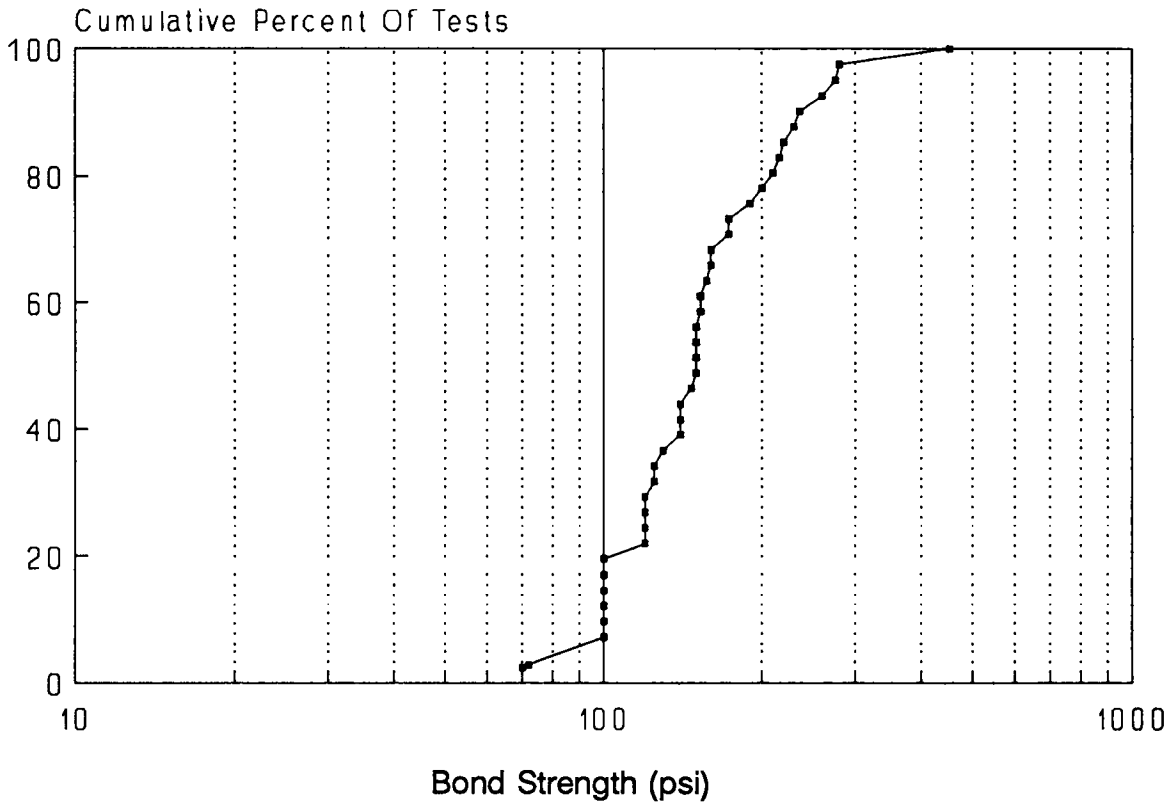

Figure 5.1 **Cumulative percentage of average bond strength results from all four bridges**

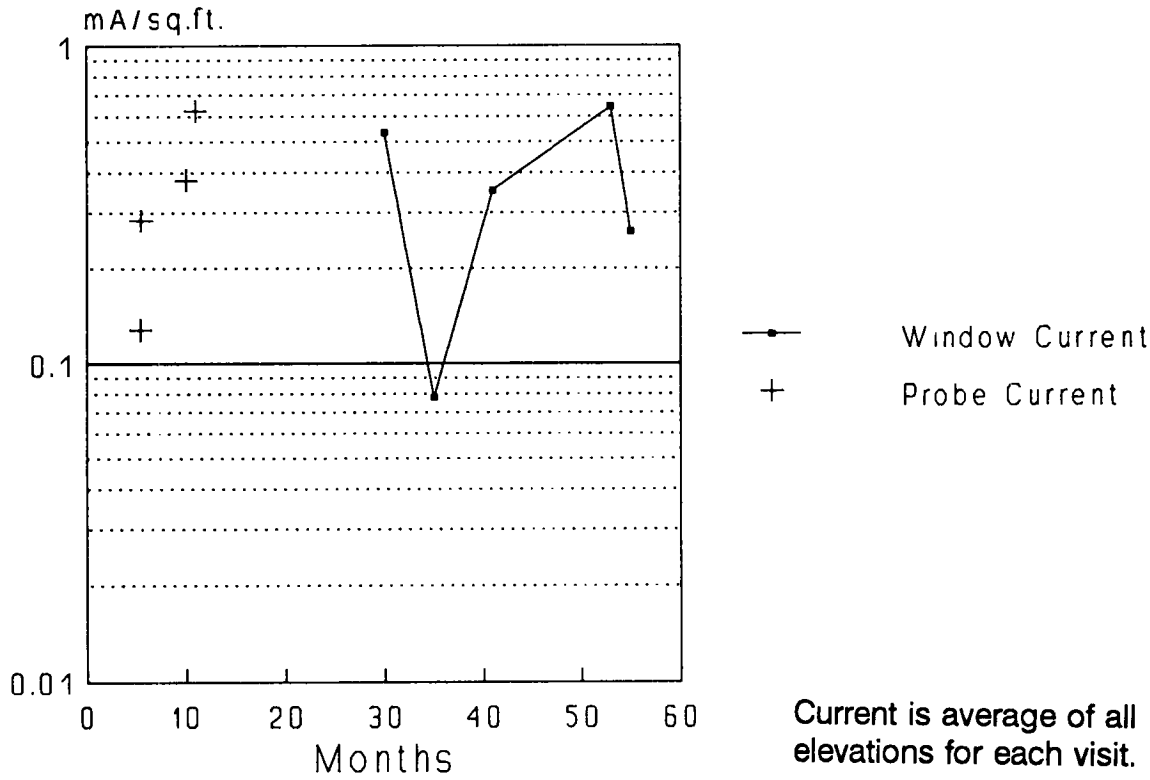

Figure 5.2 **Probe and window current density—Niles Channel Bridge (anode in service 52 months). Probe currents are for a select period when testing was performed at increased frequency**

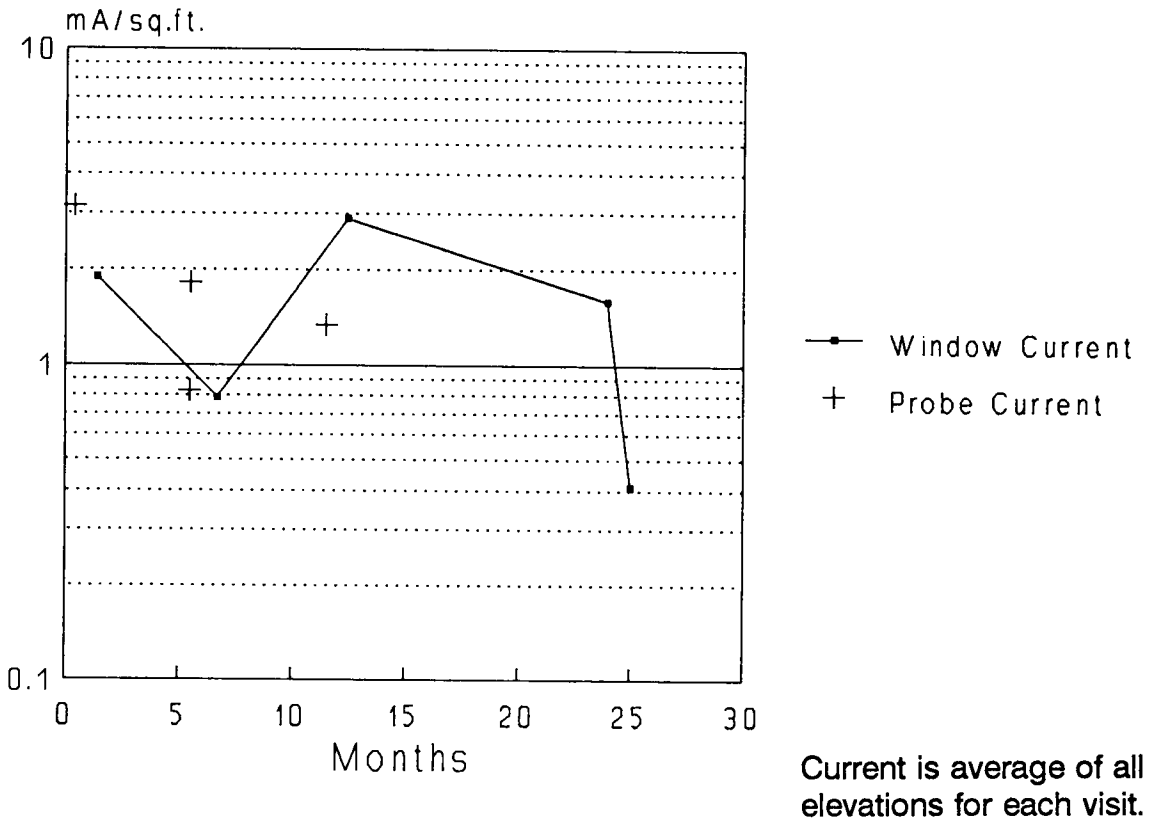

Figure 5.3 **Probe and window current density—Bahia Honda Bridge. Probe currents are for a select period when testing was performed at increased frequency**

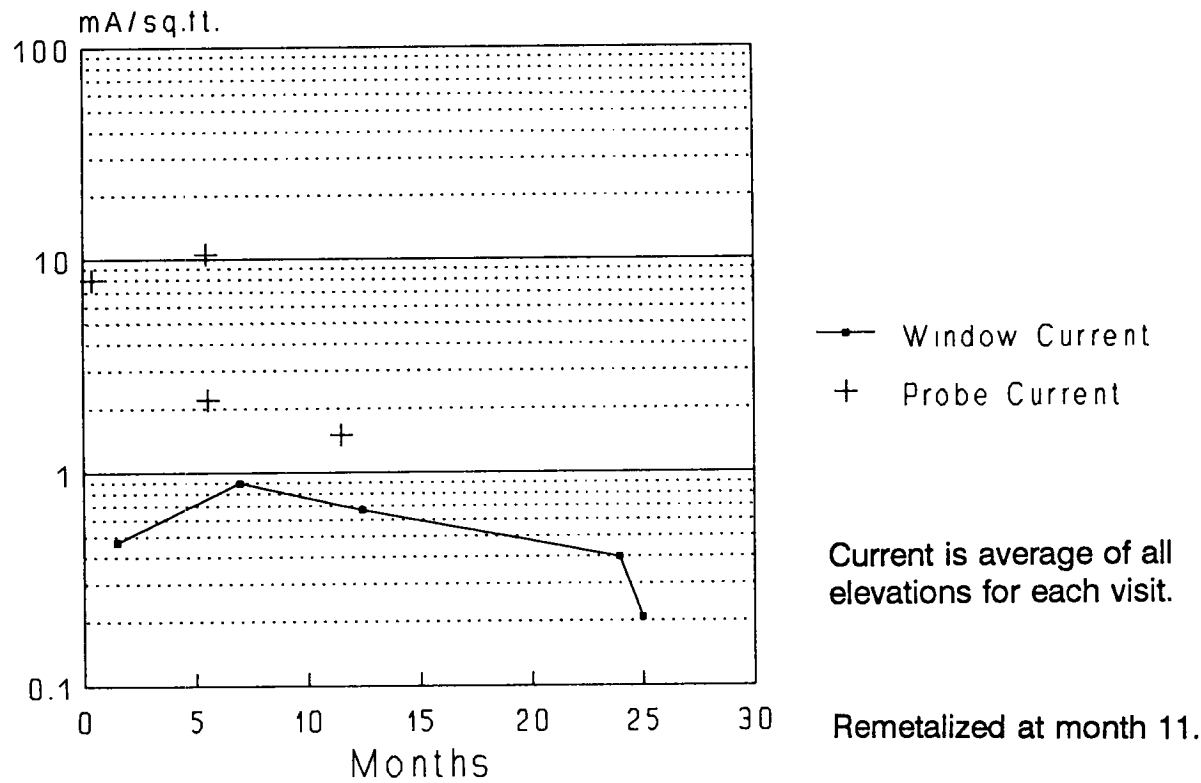

Figure 5.4 **Probe and window current density—Seven Mile Bridge. Probe currents are for a select period when testing was performed at increased frequency.**

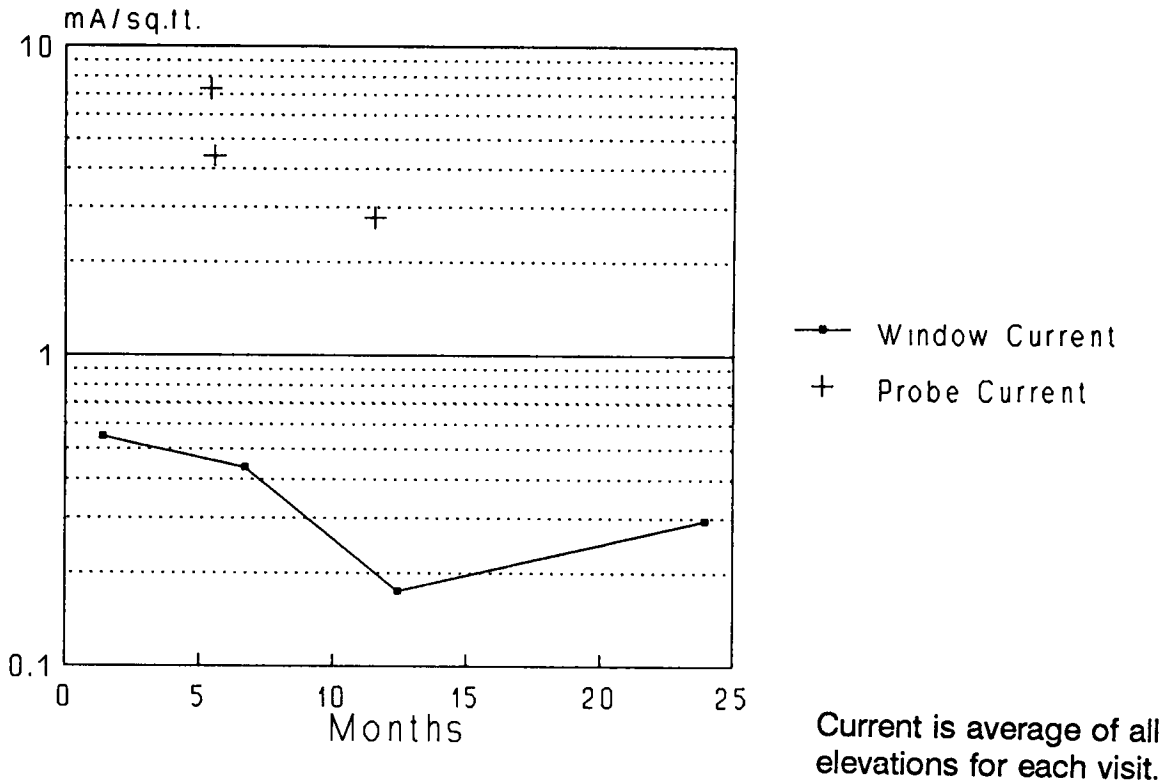

Figure 5.5 Probe and window current density—Long Key Bridge. Probe currents are for a select period when testing was performed at increased frequency.

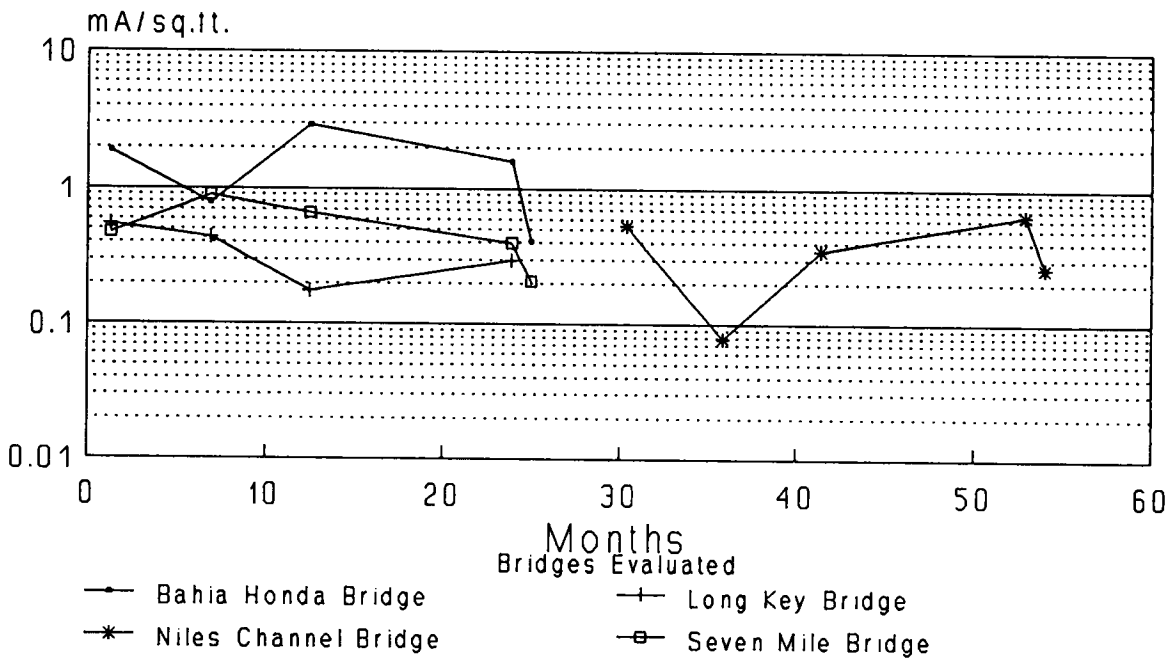

Figure 5.6 Average anode current density

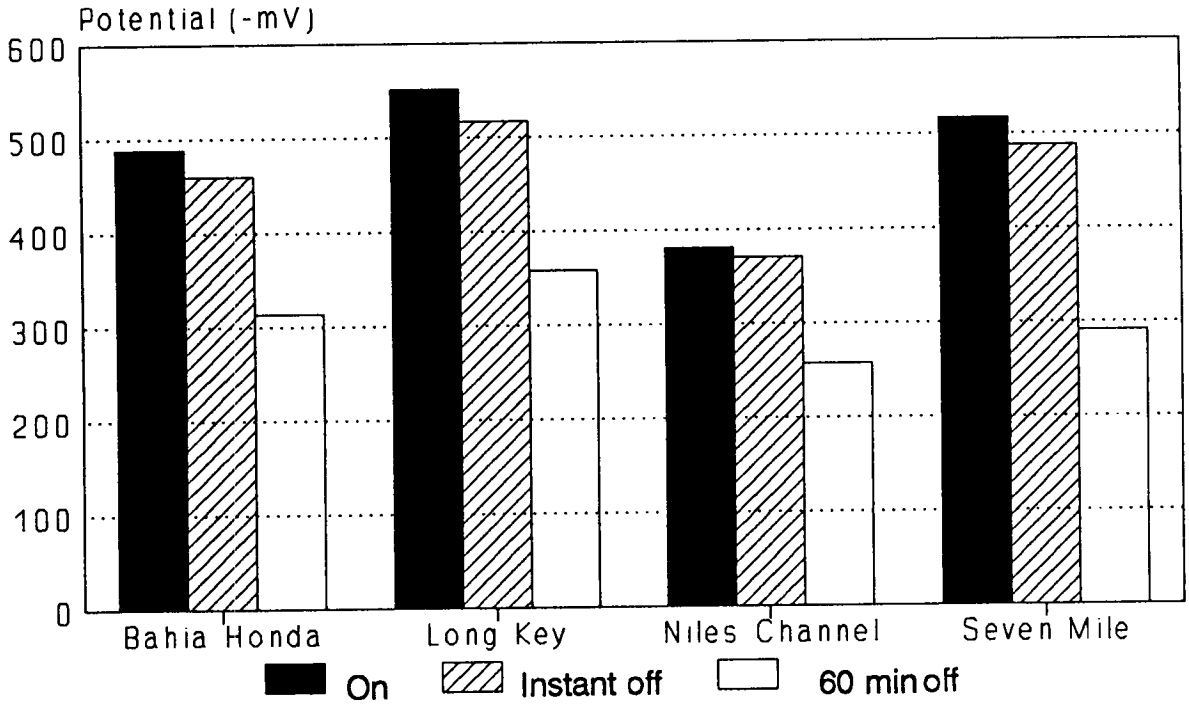

Figure 5.7 **Average polarization decay of probes. The average decay of all four bridges was 154 mV.**

6

Discussion

6.1 Field Behavior

The behavior of the metallized structures in the field has been encouraging. The coatings have remained in place and retained reasonable physical integrity after up to 4.5 years of service in the subtropical marine environment. Adhesion between the coating and the concrete has remained high. While some signs of anode wastage are evident on the oldest installations (Niles Channel), most of it is still showing significant activity.

Current density measurements on the test windows were complicated by the difficulty in maintaining reliable long-term electrical contacts. In some instances, the currents were determined indirectly by computation, from potential measurements and the known meter and inter-element resistances. Nevertheless, the results indicate that protective current delivery has been maintained over 4.5 years at about 0.5 mA/ft^2 (0.5 $\mu A/cm^2$) of concrete in structures containing corroded epoxy-coated reinforcing steel. About 1 mA/ft^2 (1.1 $\mu A/cm^2$) current delivery was obtained over 2 years on the uncoated steel Bahia Honda site. A current density of 1 mA/ft^2 (1.1 $\mu A/cm^2$) is typical for protection in mature impressed-current systems on corroded plain reinforcing steel.[28] The current delivery on corroding epoxy-coated reinforcing steel members was smaller, but quite significant considering that coated steel is involved.

While there is little evidence at this time as to the current density levels necessary to protect epoxy-coated reinforcing steel (if the protection is feasible at all), design values for corrosion of buried pipeline steel with a coating in poor condition are typically one tenth or less of those specified for bare steel.[29] The present results amply meet that criterion.

The reinforcing steel probes provided additional evidence of promising field systems performance. The average current density on the probes in the bare bar structure (Bahia

Honda) was comparable to that obtained from the adjacent anode windows (Table 5.2 and Figure 5.6).

Since the ratio of the anode surface area to that of the underlying reinforcing steel was typically near 1:1, the observations suggest that the current densities delivered by the anodes to the reinforcing steel and to the reinforcing steel probes were comparable. Therefore, it would appear that the polarized condition of the probes was a good indicator of the polarization on the reinforcing steel, at least when the reinforcing steel was uncoated.

In the structures with epoxy-coated reinforcing steel, the steel probes also gave a reasonable indication of how the anode would protect an uncoated steel system. The lower current demand of the coated steel is likely to increase the amount of protective current flowing to the probe. This increase does not appear to have been important at the Niles Channel test site, where the probe and anode current densities were comparable. However, probe current densities were noticeably larger than those of the anode at the Long Key and Seven Mile locations.

Within the limitations just discussed, the polarization decay measurements on the reinforcing steel probes (typically exceeding 100 mV over as little as 1 hour, even after many months of service) are an additional indication that considerable protection was being provided by the galvanic anode systems in the bare bar structures and that the sprayed anodes remained functional over long service times.

Indirect indication of positive protection by the galvanic anodes is also emerging. Florida Department of Transportation (DOT) maintenance records indicate that gunite repairs on other piers in the Niles Channel Bridge typically last 2 years before external signs of corrosion redevelop. Increasing damage has been reported in the piers left without any treatment. In contrast, no new cracking or other corrosion-related damage of treated piers has been observed over the past 4.5 years.

6.2 Laboratory Columns

The test results of column specimens match the behavior of the field structures. Current delivery on the order of 1 mA/ft^2 (1.1 $\mu A/cm^2$) for the region immediately above the waterline was maintained over nearly 2 years. The polarization decay for that region also consistently exceeded 100 mV in 4 hours. The galvanic anode current successfully shifted the steel macrocell current pattern, indicating efficient protection of the highest corroding element. As the system matured, current demand existed primarily in the element just above water, consistent with the expectation of conditions there being the most aggressive. The fully submerged region was expected to corrode at a very slow rate due both to poor oxygen supply and to the suppression of corrosion macrocell currents on application of cathodic protection further on the upper column.

The anodes on the chloride-free regions of the laboratory columns had very low current delivery throughout the test exposure. This was due in part to the high bulk concrete

resistivity in these areas, where the concrete was dryer. In addition, the resistance between the anode and the midpoint in these areas was significantly greater (especially when the air relative humidity was low) than the resistance between the reinforcing steel and the midpoint. These observations suggest that the current delivery of the column anode sections in the chloride-free regions was reduced by the combined effects of passivation of the zinc (no chloride ions) and the high resistance between the anode and the concrete.

Figure 6.1 summarizes the combined potential versus the current behavior of the zinc anodes (average of the three columns) over the entire test period. The three upper anodes always delivered currents less than 0.1 mA and typically about 0.01 mA (current densities of approximately 0.2 to 0.02 mA/ft^2 [0.22 to 0.022 μA/cm^2]), while maintaining potentials between -200 and -500 mV versus saturated calomel electrode (SCE). The current densities and potentials are typical of zinc in the passive condition.[30]

In contrast, the lower anode had current densities one to two orders of magnitude greater, and potentials typically in the -500 to -700 mV range versus SCE, consistent with active zinc.[30] In addition to having been placed over chloride-rich concrete (20 pcy [12 kg/m^3] initially), this anode was very close to the saltwater level.

The columns developed a ring of salt deposits 1 to 3 in. above the waterline. This ring was the result of water capillary raise and evaporation, which leads to high chloride ion accumulation in the concrete.[31] The high moisture and high chloride conditions were the main factors in retaining consistently high current delivery in that anode segment. It is also expected that similar conditions were responsible for the long-term high current delivery inferred from the field measurements.

It is also instructive to examine the average polarization conditions of the steel in the laboratory columns, as summarized in Figure 6.2 for the entire experimental record. Bar regions 1 to 3 (chloride-free concrete) showed behavior characteristic of passive steel. Bar region 4 (just above the waterline, high chloride contamination) showed low potentials and high cathodic current demand, as expected from active steel in a corrosive environment under the action of cathodic protection. Finally, the steel below the waterline showed the most negative potentials (see Figure 4.24) and current levels one or two orders of magnitude lower than region 4, oscillating between net cathodic and anodic character. As indicated earlier, this is consistent with active behavior under very limited oxygen supply and characteristic of the underwater portion of marine substructure.[32]

6.3 Compact Specimens and Anode Polarization

The behavior of the compact test specimens supported the findings indicated above but also raised some new questions.

The compact galvanic specimens in all three humidity test conditions delivered initial current densities on the order of 1 mA/ft^2 (1.1 μA/cm^2) or higher, comparable with those observed in the field and in the lower anodes on the laboratory columns. The current delivery dropped

rapidly and continually with time at 25% and 60% relative humidity, due to increases in anode-to-steel resistance associated with water loss and possible reduction in anode activity. The specimen drying is also thought to have reduced the rate of corrosion of the steel.[33] Thus, although concrete resistance and anode activity decreased with time, the extent of steel depolarization measured in the 25% and 60% relative humidity specimens was still significant (Table 4.1).

The current delivery in the specimens at 85% relative humidity also decreased rapidly and continually with service time. The current decrease was also associated with decreasing amounts of steel depolarization. This indicated that the current decrease was due to increasingly poorer performance of the protecting system, and not to less demand on the part of the steel (less demand could have been expected if, over time, the cathode current had created a substantial decrease in chloride content around the steel). Further evidence of the decay in performance was that, after long exposure, the steel potential was about the same as the disconnected control specimens.

The anode-to-steel resistance in the compact specimens at 85% relative humidity changed relatively little during the test. Moreover, the resistance between the anode and specimen midpoint was always comparable to that between the steel and midpoint. This suggests that the decay was not due to the simple buildup of a resistive material between anode and concrete, as may have been in the case for the anode patches on the chloride-free portion of the test columns.

Microstructural examination of the zinc-concrete interface revealed that, although some wastage had taken place, significant amounts of unreacted zinc remained on the anode after the current delivery had dropped (Figure 4.13). Therefore, anode wastage did not appear to be the cause of the decay. Further examination showed no conclusive evidence of the formation of a poor conductance zone between the anode and the concrete, thus supporting the conclusions suggested by the resistance measurements.

6.4 Surface Wetting of the Anodes

Examination of the remaining possible causes of current decay in the compact specimens suggested that the absence of direct wetting of the anode surface was a key factor. Both the laboratory columns and the field installations had better long-term current delivery, and both contained anode portions that were in direct contact with saltwater at least some of the time. The momentary wetting of the compact specimens resulted in a large momentary increase in current delivery. Current increases were also observed even when the anodes in the chloride-free portions of the laboratory columns were wetted with distilled water (Figure 4.28).

These observations confirm the importance of direct surface wetting on increasing anode current delivery. The precise mechanism by which this takes place is not known at this time. One possibly important factor is an increase of the fraction of the anode surface in direct contact with electrolyte upon wetting. This is likely since, even in an apparently dry anode, a certain amount of condensed water must exist within the fine porosity of the anode and the

concrete due to capillary depression of the local equilibrium vapor pressure. Thus, the anode delivers current at an effective rate consistent with the fraction of metal surface in contact with electrolyte. Upon wetting, the fraction would increase sharply with consequent increase in current delivery.

The anode-to-concrete resistance and its variation upon wetting is also expected to play some role on the extent of current delivery. As shown in the previous section, that role may not be very important in the case of the compact specimens in the 85% relative humidity environment. Moreover, in both the 85% and 60% relative humidity compact specimens the anode-to-midpoint resistance values did not vary significantly upon temporary wetting. On the other hand, the anode-to-midpoint resistance in the chloride-free portion of the laboratory columns (in room air) was much greater than the anode-to-midpoint resistance of the compact specimens exposed to 60% relative humidity (also room air). The anode-to-midpoint resistance in the columns was also much more sensitive to wetting than that of the compact specimens. This difference in behavior appears to be the result of the compact specimen concrete being rich in chloride ions (from the salting procedure). While the increase in conductivity due to chloride contamination is moderate in bulk concrete,[34] the effect can be important if some concrete carbonation or anodic acidification had taken place directly below the zinc coating during service. In carbonated or otherwise reduced-Ph concrete the conductivity of the chloride-free pore solution can be very low, and, in that case, the differences due to chloride contamination would likely be more notable.[34] Therefore the electrolyte in the pores of the concrete, in direct contact with the zinc, might be expected to be much more conductive in the compact specimens than in the chloride-free portion of the columns. A related factor is that the presence of hygroscopic salts at the concrete surface could increase the equilibrium amount of water present at the anode-concrete interface. In summary, anode-to-concrete resistance in the chloride-contaminated specimens appears to be low enough (with or without direct surface wetting) that current limitation occurs by other mechanisms. In the chloride-free surfaces reduction of anode-to-concrete resistance by direct wetting may be an important factor in increasing current delivery.

Surface wetting also resulted in sharp negative excursions of the anode potential during wetting. These effects could have resulted from solution dilution with consequent lowering of the zinc/zinc ion redox potential, phenomena involving loss of passivity in previously wetted surfaces, and the behavior of freshly wetted portions of the metal surface. The complicated interplay of surface electrochemical behavior, ohmic changes, and the amount of wetted surface area cannot be determined with the information available.

The experiments with impressed anodic currents provided results consistent with the behavior of the galvanic specimens. As would be expected, the driving potential had to be moved in the positive direction to compensate for the increasing polarization of the anode. The effect in the low-humidity environment agrees with the behavior observed in field impressed-current systems using sprayed zinc anodes.[15]

While no wetting tests were performed on the impressed current specimens in the high-humidity environment, it is expected that the potential demand would have decreased significantly upon wetting. In general, the field and laboratory tests indicated that performance of galvanic anodes is likely to be best under conditions where direct wetting

occurs. Thus, the concept is promising for protecting the splash zone on marine substructure components, which are the areas that most often need corrosion protection.

6.5 Durability and Materials

There were considerable problems in maintaining good lead-to-anode contacts in the impressed-current specimens, to the extent that the results of those tests do not allow accurate evaluation of the durability of the anode itself.

Continued evaluation of the long-term performance of the field installations appears to be the best measure of the durability. The observation at Niles Channel over 4 years is encouraging. The results suggest that zinc spray is significantly superior to conventional gunite patching as a rehabilitation tool in this environment.

The experiments were inconclusive on the use of an organic topcoat over the anode, as there was no clear evidence of changes in the long-term polarization behavior of the coated versus uncoated anodes.

The impressed-current experiments suggested that the driving potential requirement of the 85% Zn-15% Al anodes was about 200 mV lower than that of the regular zinc anodes. That potential difference, if consistently attainable, could create a substantial increase in the current delivery ability during galvanic operation.

A new series of galvanic tests is in progress to compare the behavior of pure versus alloyed zinc anodes and the effects of surface wetting. The results will be presented in a future publication.

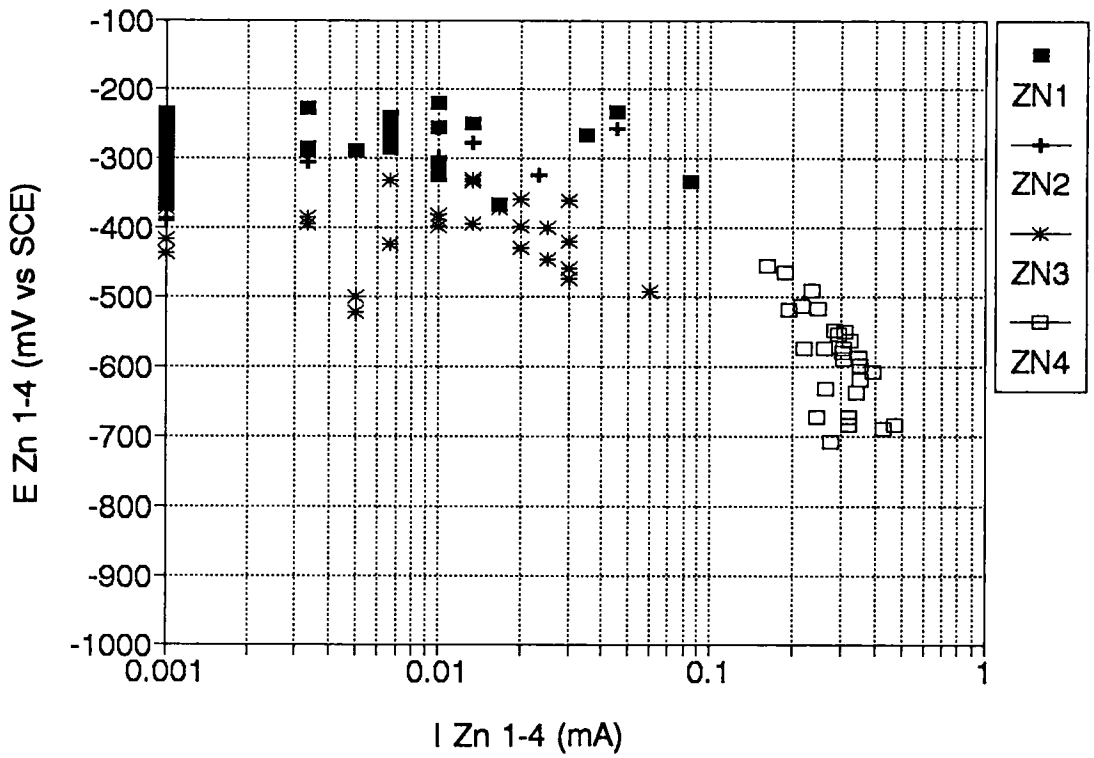

Figure 6.1 **Average polarization behavior of the anodes of the laboratory columns throughout the entire exposure period. All currents are anodic.**

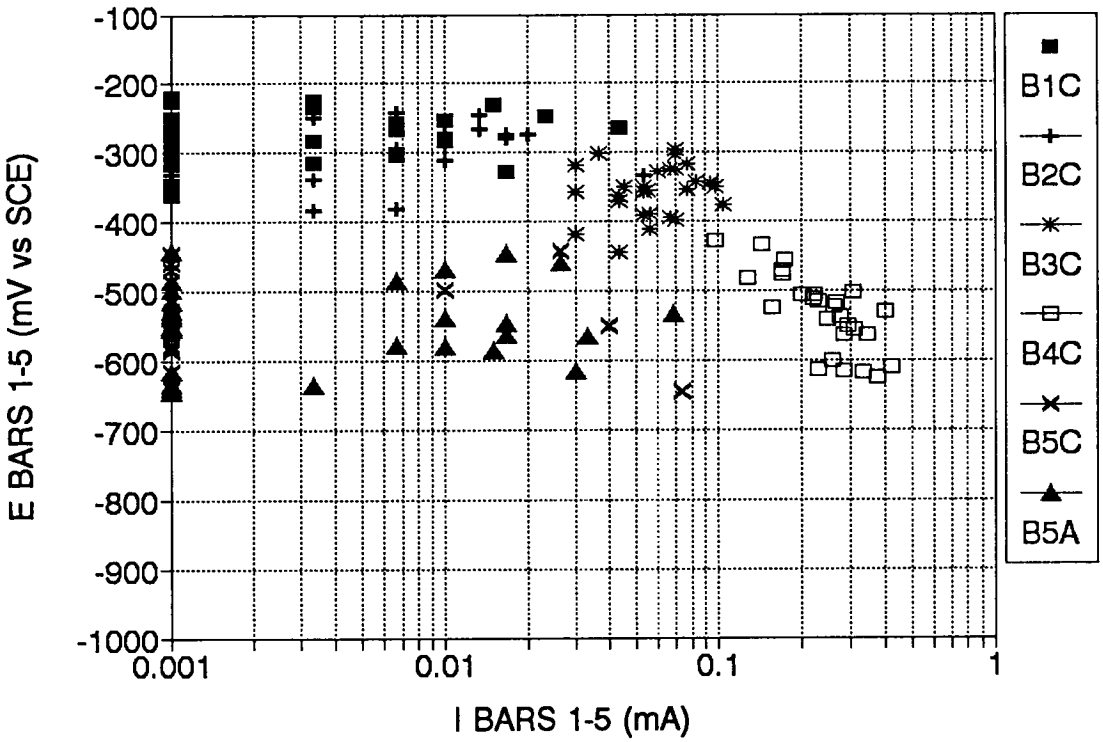

Figure 6.2 **Average polarization behavior of the steel bars of the laboratory columns throughout the entire exposure period when the anodes were operational. Currents indicated by C are cathodic; by A (observed only at level 5) are anodic.**

7

Conclusions

1. The galvanic anodes were installed on marine bridge substructures in a subtropical environment rapidly and economically with existing technology.

2. The anodes have continued to show physical integrity after up to 4.5 years of service in a harsh marine environment.

3. Field current density measurements over 4.5 years indicate that typically 0.5 mA/ft^2 (0.54 $\mu A/cm^2$) has been maintained on structures containing corroded epoxy-coated rebar. On the order of 1 mA/ft^2 (1.1 $\mu A/cm^2$) was maintained over 2 years on structures containing corroded ordinary rebar.

4. Rebar probe measurements consistently showed typical steel polarization decay values that exceeded 100 mV in as little as 1 hour.

5. Anodes placed near the waterline on laboratory test columns replicated the current delivery and polarization decay observed on the field structures. Anodes placed in dryer, chloride-free portions of the same columns did not contribute significantly to the overall protection.

6. After nearly 2 years of testing, the current density delivery by the active anodes in the laboratory was on the order of 1 mA/ft^2 (1.1 $\mu A/cm^2$). Steel polarization decay in the area of expected highest corrosion continued to exceed 100 mV within 4 hours.

7. The compact laboratory specimens exposed to medium (near 60%) and low (near 25%) relative humidity environments showed significant and continuous decreases in current delivery as a function of time. The decrease was more pronounced in dryer environments. However, appreciable amounts of steel polarization decay were attained

with these specimens, probably because the corrosion rate of the steel is much lower in dry concrete.

8. The compact laboratory specimens placed in the 85% relative humidity test environment also showed a pronounced decrease in current delivery with time. Steel polarization decay test results indicated a corresponding reduction of protection of the steel in these specimens.

9. The loss of efficiency in the compact laboratory specimens in the 85% relative humidity environment was primarily a consequence of long-term polarization of the anode. Polarization of the steel, increase in concrete resistance, and anode wastage were found to be of only secondary importance in causing the long-term loss of efficiency.

10. Current delivery on the compact specimens exposed to 85% relative humidity and on the laboratory columns was increased dramatically by direct wetting of the anode surface. Direct wetting of the anode (by seawater splashing or misting in the field, or by capillary rise in laboratory columns) may be a key factor in achieving high protective current delivery.

11. There was no significant change in the polarization behavior of the anodes as a result of the presence of an organic topcoat.

12. In impressed-current tests, the driving potential requirement to achieve 1 mA/ft^2 (1.1 $\mu A/cm^2$) was less (by about 200 mV) for the 85% Zn-15% Al anodes than for the commercially pure zinc anodes.

13. The results support the use of the sprayed galvanic anode technique for locations such as the splash-evaporation zone of marine bridge substructures, where high relative humidities and intermittent wetting of the surface are prevalent (usually coinciding with the region in greatest need of corrosion protection).

8

References

1 J. Slater, "Corrosion of Metals in Association with Concrete," ASTM Special Technical Publication 818, ASTM, Philadelphia (1983).

2 M. Makita, Y. Mori, and K. Katawaki, "Marine Corrosion Behavior of Reinforced Concrete at Tokyo Bay," ACI Publication SP-65, p. 271, in *Performance of Concrete in Marine Environments*, V. Malhotra, ed., ACI, Detroit (1980).

3 G. Geimar, "Repair of Concrete in Tropical Marine Environment," ibid., p. 527.

4 R. Powers, and R. Kessler, "Corrosion Evaluation of Substructure, Long Key Bridge," Corrosion Report No. 87-9A, Florida Department of Transportation, Gainesville, FL (1987).

5 A. Zayed, A. Sagüés, and R. Powers, "Corrosion of Epoxy-Coated Reinforcing Steel in Concrete," Paper No. 379, *Corrosion*/89, National Association of Corrosion Engineers, Houston (1989).

6 R. Kessler, and R. Powers, *Materials Performance*, Vol. 28, No. 9, p. 24 (1989).

7 C. Mudd, G. Mussinelli, M. Tettamanti, and P. Pedeferri, "New Developments in Mixed Metal Oxide Activated Net for Cathodic Protection of Steel in Concrete," Paper No. 168, *Corrosion*/89, National Association of Corrosion Engineers, Houston (1989).

8 C. Mudd, G. Mussinelli, M. Tettamanti, and P. Pedeferri, *Materials Performance*, Vol. 27, No. 9, p. 18 (1988).

9 B. Wyatt, and D. Irvine, *Materials Performance*, Vol. 26, No. 12, p. 12 (1987).

10 D. Jackson, "The Cost-Benefits of Cathodic Protection for Reinforced Concrete Bridge Decks," Paper No. 80, *Corrosion*/82, National Association of Corrosion Engineers, Houston (1982).

11 D. Whiting, D. Stark, and W. Schutt, *Galvanic Cathodic Protection for Reinforced Concrete Bridge Decks*, National Cooperative Highway Research Program, Report No. 234, Transportation Research Board, National Research Council, Washington, DC (June 1981).

12 O. Rincon, and C. Locke, "Experience with Cathodic Protection of Bridge Pilings in Lake Maracaibo," Paper No. 260, *Corrosion*/85, National Association of Corrosion Engineers, Houston (1985).

13 W. Hartt, and R. Brown, "Cathodic Protection of Steel in Concrete," Preprint No. 6, in *Solving Rebar Corrosion Problems in Concrete*, published by National Association of Corrosion Engineers, Houston (1983).

14 V. Chaker, and D. Lindemuth, "The State of the Art in Corrosion Protection of Marine Piles," Paper No. 376, *Corrosion*/90, National Association of Corrosion Engineers, Houston (1990).

15 R. Carello, D. Parks, and J. Apostolos, *Development, Testing and Field Application of Metallized Cathodic Protection Coatings on Reinforced Concrete Substructures*, Report No. FHWA/CA/TL-89/04, National Technical Information Service, Springfield, VA (1989).

16 H.M. Laylor, Oregon Department of Transportation, personal communication, 1993.

17 R. Kessler, and R. Powers, "Zinc Metallizing for Galvanic Cathodic Protection of Steel Reinforced Concrete in a Marine Environment," Paper No. 324, *Corrosion*/90, National Association of Corrosion Engineers, Houston (1990).

18 B. Shaw, and P. Moran, *Materials Performance*, Vol. 24, No. 11, p. 22 (1985).

19 H. Herman, and K. Altorfer, "Zinc Thermal Spray Metallizing for Corrosion Protection of Structural Steel."

20 H. Morrow, *Journal of Protective Coatings and Linings*, Vol. 4, No. 1, p. 39 (1987).

21 *Metallinze* (The Corrosion Metallizing Bulletin), Vol. 4, No. 3, p. 1 (1988).

22 K. Chandler, *Marine and Offshore Corrosion*, Butterworths, London (1985).

23 D. Nevison, "Corrosion of Zinc," in *Metals Handbook*, Vol. 13, *Corrosion*, p. 755, ASM International, Metals Park (1987).

24 M. Peterson, and J. Lennox, *Materials Performance*, Vol. 23, No. 3, p. 15 (1984).

25 I. Cornet, and B. Bresler, *Galvanized Steel in Concrete: Literature Review and Assessment of Performance*, International Lead Zinc Research Organization, New York (1981).

26 S.G. Millard, M. Ghassemi, J. Bungey, and M. Jafar, "Assessing the Electrical Resistivity of Concrete Structures for Corrosion Durability Studies," in *Corrosion of Reinforcement in Concrete*, C. Page, K. Treadaway, and P. Bamforth, eds., p. 303, Elsevier Applied Sciences, London (1990).

27 A. Sagüés, "Corrosion Measurements Techniques for Steel in Concrete," Paper No. 353, *Corrosion*/93, National Association of Corrosion Engineers, Houston (1993).

28 *Control Criteria and Materials Performance Studies for Cathodic Protection of Reinforced Concrete*, Report No. SHRP-S-670, Strategic Highway Research Program, National Research Council, Washington, DC (1993).

29 M. Fontana, *Corrosion Engineering*, 3rd. ed., McGraw-Hill, New York (1986).

30 M.C. Andrade, and A. Macias, "Galvanized Reinforcements in Concrete," Chapter 5 in *Surface Coatings-2*, A. Wilson, J. Nicholson, and H. Prosser, eds., Elsevier Applied Sciences, London (1988).

31 A. Aguilar, A. Sagüés, and R. Powers, "Corrosion Measurements of Reinforcing Steel in Partially Submerged Concrete Slabs," in *Corrosion Rates of Steel in Concrete*, N. Berke, ed., STP 1065, ASTM, Philadelphia (1990).

32 S.C. Kranc, and A. Sagüés, "Computation of Reinforcing Steel Corrosion Distribution in Concrete Marine Bridge Substructures," Paper No. 327, *Corrosion*/93, National Association of Corrosion Engineers, Houston (1993).

33 C. Andrade, M. Cruz Alonso, and J. Gonzalez, "An Initial Effort to Use the Corrosion Rate Measurements for Estimating Rebar Durability," in *Corrosion Rates of Steel in Concrete*, ASTM STP 1065, N. Berke, V. Chaker, and D. Whiting, eds., ASTM, Philadelphia (1990).

34 S. Goñi, A. Moragues, and M.C. Andrade, "Influence of the Conductivity and the Ionic Strength of Synthetic Solutions Which Simulate the Aqueous Phase of Concrete in the Corrosion Process," *Materiales de Construcción*, Vol. 39, p. 19 (1989).